1950

Range-energy studies of fission fragments

Robert Briggs Leachman
Iowa State College

INFORMATION TO USERS

This manuscript has been reproduced from the microfilm master. UMI films the text directly from the original or copy submitted. Thus, some thesis and dissertation copies are in typewriter face, while others may be from any type of computer printer.

The quality of this reproduction is dependent upon the quality of the copy submitted. Broken or indistinct print, colored or poor quality illustrations and photographs, print bleedthrough, substandard margins, and improper alignment can adversely affect reproduction.

In the unlikely event that the author did not send UMI a complete manuscript and there are missing pages, these will be noted. Also, if unauthorized copyright material had to be removed, a note will indicate the deletion.

Oversize materials (e.g., maps, drawings, charts) are reproduced by sectioning the original, beginning at the upper left-hand corner and continuing from left to right in equal sections with small overlaps.

ProQuest Information and Learning
300 North Zeeb Road, Ann Arbor, MI 48106-1346 USA
800-521-0600

RANGE-ENERGY STUDIES OF FISSION FRAGMENTS

by

Robert Briggs Leachman

A Dissertation Submitted to the
Graduate Faculty in Partial Fulfillment of
The Requirements for the Degree of
DOCTOR OF PHILOSOPHY

Major Subject: Physics

Approved:

Signature was redacted for privacy.

In Charge of Major Work

Signature was redacted for privacy.

Head of Major Department

Signature was redacted for privacy.

Dean of Graduate College

Iowa State College

1950

UMI Number: DP12048

ProQuest Information and Learning Company
300 North Zeeb Road
P.O. Box 1346
Ann Arbor, MI 48106-1346

TABLE OF CONTENTS

INTRODUCTION

When a heavy nucleus captures a neutron and undergoes fission two heavy fragments are emitted with large kinetic energy. It is the purpose of this investigation to determine the change in the kinetic energy of U^{238} fission fragments along their path while being stopped in various gasses.

Since fission fragments are very heavy and energetic, they are initially stripped of some orbital electrons. As the fragments are slowed along their path, they gradually take on these electrons. This changing effective charge has an important effect on the rate of energy loss along the path of a fragment. In this respect, good range-energy data for fission fragments and their explanation are expected to give a deeper insight into the general energy loss process of atomic particles. Earlier investigations of the energy loss process have been based on the simpler problem of light particles such as alpha-particles and protons, which are completely ionized over most of their range.

Moreover, the large mass of fission fragments makes possible a study of nuclear collision energy loss that is not feasible with light particles. The energy lost by nuclear collisions, as distinguished from energy lost by electronic collisions, becomes important as the fragment

acquires its final orbital electron. Because of their large mass, fission fragments at this point in their range have kinetic energy which is not negligible compared to the initial kinetic energy. On the other hand, the energy lost by light particles in nuclear collisions is negligible.

Although only limited velocity-range data on fission fragments were available at the time, the energy loss problem was treated theoretically by Knipp and others[1] and by Bohr[2] shortly after the discovery of fission. These calculations were based on an energy loss rate proportional to the square of the effective fission fragment charge, which was determined from the Thomas-Fermi model of the atom. Further refinements in these calculations require accurate and more complete experimental data.

Experimental Methods

Fission fragment energy measurements are much more difficult than measurements of the light particles, which have a constant effective charge over most of their range and a definite mass. These constants make possible precise

---

[1] J. K. Knipp and E. Teller, Phys. Rev. 59, 659 (1941); J. H. M. Brunings, J. K. Knipp and E. Teller, Phys. Rev. 60, 657 (1941).

[2] N. Bohr, Phys. Rev. 58, 654 (1940); N. Bohr, Phys. Rev. 59, 270 (1941).

measurements of light particle energy by electrostatic or magnetic deflection. Since fission fragments have varying effective charge and have a wide distribution of mass, they are not conveniently measured by such means.

The more accurate measurements of the fragment energy are based on a determination of the number of ion pairs formed in a stopping gas with the assumption that this number is proportional to the energy loss. Using a shallow ionization chamber, Lassen[3] has measured the linear rate of ion pair formation in small range intervals along the path of fragments in various gasses. Since this ionization rate varies with different fragments, his data of the ionization rate over the total range are not of individual fragments, but of the average rates for the heavy and light fragments. West[4] used a shallow chamber and measured ionizations formed in various ranges, always including the origin of the track. His range-ionization data also are not of individual fragments. Demers[5] used grain density measurements of tracks in photographic plates to give rather limited ionization rate data on individual fragments.

---

[3] N. O. Lassen, Kgl. Danske Vid. Sels. Math.-Fys. Medd. 25, No. 11 (1949).

[4] D. West, Can. J. Research, Sect. A 26, 115 (1948).

[5] P. Demers, Phys. Rev. 70, 974 (1946).

The method of range-ionization measurement of interest in this investigation is electron collection from ionization chambers as used by Sherr and Peterson[6] to obtain data on eight fragments stopped in argon. This method involves the study of voltage waveforms from ionization chambers, within which the fragments are stopped. Data are given on individual fragments, but the errors due to ion recombination, electron diffusion, and electronic effects have received little consideration.

Plan of Investigation

The objects of this investigation are: (1) to study the energy-ionization relation necessary for a conversion of the experimental range-ionization data to range-energy information, (2) to obtain accurate range-ionization data of fission fragments in various gasses by the electron collection method, (3) to use the electron collection with each chamber of "back-to-back" ionization chambers in order to observe simultaneously the range-ionization of fission fragment pairs, and (4) to study the influence of ion recombination and electron diffusion on the experimental data.

---

[6] R. Sherr and R. Peterson, Rev. Sci. Inst. 18, 567, (1947).

Since adequate data on the distributions in fission fragment mass and total ionization have been published, the energy-ionization study to follow is confined to a mathematical treatment of these distributions. Efforts to improve the experimental range-ionization data are directed towards raising the signal/noise ratio and improving the electronic method of differentiation. A comparison of range-ionization data for fragments stopped in different pressures of gas is expected to reveal distortions in the data due to ion recombination. Although the electron collection method gives a rough measure of the electron diffusion, a more complete understanding of the diffusion effect on data is to be expected from a theoretical treatment.

ENERGY-IONIZATION RELATION

Although an early calorimetric experiment[7] measured the total fission energy, including kinetic energy and some radiation energy, the variations of fragment mass and effective charge have prevented direct measurement of the exclusively kinetic energy. The numbers of ion pairs produced by stopping fragments have been measured, but these data are difficult to interpret in terms of energy; the data are generally reported with an energy conversion involving simply the energy/ionization ratio found for alpha-particles of known energy. The fragment mass distributions inferred from these ionization data[8,9] are not the same as the mass distributions obtained by direct measurement[10]. In this section a general method of comparing ionization and mass distributions is given, from which may be evaluated the two principal sources of the discrepancy. These are (a) the energy dispersion and (b) the lack of precise proportionality between the measured ionization and the

---

[7] M. C. Henderson, Phys. Rev. 58, 774 (1940).

[8] D. C. Brunton and W. B. Thompson, Phys. Rev. 76, 848 (1949).

[9] M. Deutsch and M. Ramsey, MDDC 945 (1946).

[10] Plutonium Project, Rev. Mod. Phys. 18, 513 (1946); E. P. Steinberg, J. A. Seiler, A. Goldstein and A. Dudley, MDDC 1632 (1947).

ionization energy (i.e. the energy required by a fission fragment of a particular mass to produce the measured ionization).

The energy dispersion (a) is the distribution of the energy deviations between the initial energy (i.e. the fragment kinetic energy before neutron emission) and the ionization energy. The deviations are a combination of instrumental errors of ionization measurement and of the recoil energy of the fragments due to prompt neutron emission. The distribution in initial energy, obtained from the mass distribution and the momentum condition, is distorted into the ionization energy distribution by the energy dispersion. The relative variation (b) in the fragment energy/ionization ratio, assumed to be the principal remaining cause for the difference between the mass and ionization distributions, is determined by a comparison of the distributions in ionization energy and measured ionization.

It is noted that the addition of the energy dispersions for the fragments of binary fission pairs is a not negligible contribution to the observed distribution[11] in the total ionization of pairs.

---

[11] D. C. Brunton, Phys. Rev. 76, 1798 (1949).

Procedure

Using L and H to indicate the light and heavy fragment we designate:

E_L, E_H = initial kinetic energies

I_L, I_H = measured ionizations (including effects of instrumental errors and recoil energy)

$w_L I_L$, $w_H I_H$ = ionization energies;

and for fragment pairs,

$$R_E = \frac{E_L}{E_H}$$

$$R_I = \frac{I_L}{I_H}$$

$$R = \frac{w_L I_L}{w_H I_H} = \frac{w_L}{w_H} R_I$$

$$E = E_L + E_H$$

$$I = I_L + I_H$$

$$W = w_L I_L + w_H I_H,$$

where w_L and w_H are the true energy/ionization ratios varying with fragment mass.

The distortion of the initial energy distribution into the ionization energy distribution by the energy dispersion can be expressed in these parameters. The distribution P of the total ionization energy W and ionization energy ratio R is related to the distribution P_E of the total initial energy E and initial energy ratio R_E by the dispersion

function D in the equation

$$P(R,W) = \int_0 dE \int_0 dR_E D(R_E,E;R-R_E,W-E)P_E(R_E,E), \qquad (1)$$

where all functions are normalized to unity.

The distribution P_E is obtained from a fragment mass distribution by the momentum relation $m_L E_L = m_H E_H$, which is the equation for binary fission before neutron emission. It is known that a compound nucleus generally divides into two unequal[10] fragments and from the moving[12] fragments an average total[13] of from one to three neutrons are promptly emitted. A good determination of the $\frac{m_H}{m_L}$ distribution for U^{235} slow neutron fission can be obtained by adding the mass of half of the neutrons to each of the complementary masses of the distribution of the final masses (masses after neutron emission) and forming the distribution of the ratio. Since the neutrons come from opposite fragments twice as frequently as from the same[14] and since the mass of these neutrons is much less than the fragment mass, the error involved in this neutron mass assignment is small. The distribution in $\frac{m_L}{m_H}$ is then the

---

[12] R. R. Wilson, Phys. Rev. 72, 189 (1947).

[13] H. D. Smythe, Atomic Energy for Military Purposes (Princeton University Press, Princeton, 1945).

[14] S. DeBenedetti, J. E. Francis, Jr., W. M. Preston, and T. W. Bonner, Phys. Rev. 74, 1645 (1948).

desired distribution $P_E(R_E)$, but without associated energy data the E dependence of P_E cannot be determined. This $P_E(R_E)$ distribution is shown in Fig. 1.

With these limited data Eqn. (1) is reduced to

$$P(R) \cong \int_0^\infty dR_E \; D_r \; (R_E, \bar{E}; R-R_E) P_E(R_E), \qquad (2)$$

where

$$P_E(R_E) = \int_0^\infty dE \; P_E(R_E, E)$$

$$P(R) = \int_0^\infty dW \; P(R, W)$$

$$D_r(R_E, \bar{E}; R-R_E) = \int_0^\infty dW \; D(R_E, \bar{E}; R-R_E, W-\bar{E}),$$

and $\bar{E}$ is some suitably chosen average value of the total kinetic energy. Various reasonable methods of averaging E are found to change D_r only slightly, thus the distribution P(R) is quite insensitive to the averaging. D_r is the ratio dispersion function, which is determined later.

Although the ionization data are available as a distribution $P_I(R_I, I)$, the limitation to P(R) allows its comparison with only $P_I(R_I)$, where

$$P_I(R_I) = \int_0^\infty dI \; P_I(R_I, I).$$

The distribution $P_I(R_I)$ found by two experiments[10,15] on U^{235} slow neutron fission is shown in Fig. 1. This limitation allows a determination of the variations of the ratio $\frac{W_L}{W_H}$, but not of absolute magnitudes. For the normalized distributions $P_I(R_I)dR_I = P(R)dR$, from which

---

[15] D. C. Prunton and G. C. Hanna, Can. J. Research, Sect. A. 28, 190 (1950).

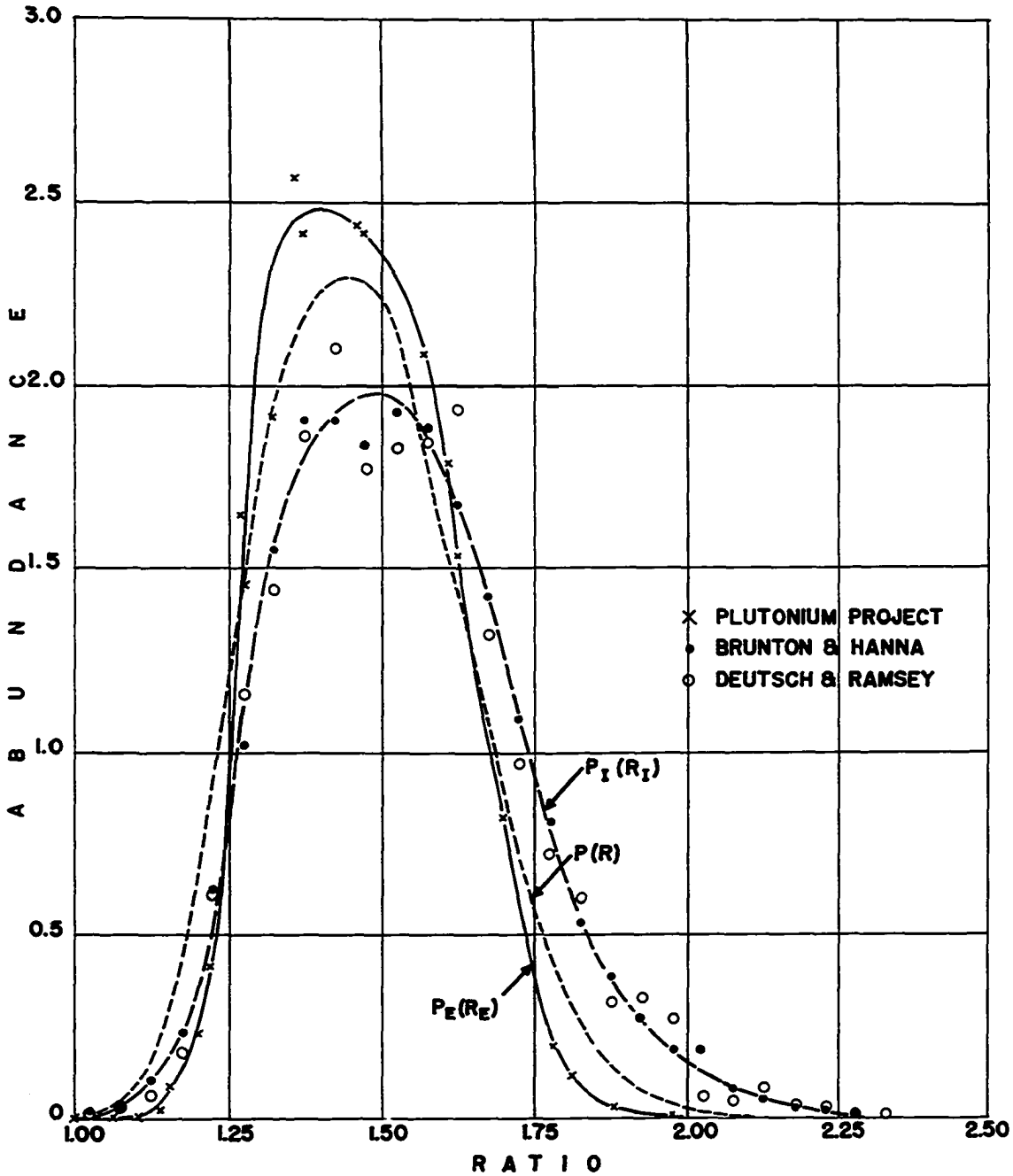

Fig. 1. Normalized ratio distributions of U^{235} fission fragments.

is obtained

$$P_I(R_I) = P\left(\frac{w_L}{w_H} R_I\right)\left[\frac{w_L}{w_H} + \alpha R_I\right], \qquad (3)$$

where $\alpha = \frac{d}{dR_I}\left(\frac{w_L}{w_H}\right)$. Eqn. (3) indirectly expresses $\frac{w_L}{w_H}$ as a function of R_I.

Actually, the distribution $P_E(R_E)$ is first changed by the dispersions due to recoil and some instrumental errors. The other instrumental errors have the effect of changing the true $P_I(R_I)$ distribution into the observed distribution. However, a combined dispersion D_r acting on $P_E(R_E)$ gives essentially the same results. Limited experimental data on these dispersions are available from which the combined dispersion D_r can be estimated. An alternative determination of D_r is afforded by an analysis of $P_I(R_I)$ and P(R) in the region of symmetrical fission. It is to be expected[16] that w be a slowly varying function of the fission asymmetry such that $\frac{w_L}{w_H}$ as a function of R_I approaches unity linearly as R_I approaches unity. The dispersion is determined analytically by finding a D_r giving the proper P(R) by means of Eqn. (2). The proper P(R) is related to the experimental $P_I(R_I)$ by Eqn. (3) with the linearity requirement that α be nearly constant and $\frac{w_L}{w_H} = 1 + \alpha(R_I - 1)$.

---

[16] N. Bohr, Kgl. Danske Vid. Sels. Math.-Fys. Medd. 18, No. 8 (1948).

The effect of three different dispersion functions to be discussed later is illustrated in the region of symmetrical fission by Fig. 2. The use of a relatively narrow dispersion function gives the P(R) distribution labeled $\Delta r = 0.10$; it can fit the experimental $P_I(R_I)$ data only when a fluctuating value of α is used. Indeed, α must be positive at ratios below 1.2 and negative at greater ratios. A broader dispersion function gives the P(R) distribution labeled $\Delta r = 0.18$; it requires a negative α of large value near unity ratio but of small value at ratios greater than 1.1. A dispersion function of intermediate width gives the P(R) distribution labeled $\Delta r = 0.14$; it gives a reasonably good fit when the value $\alpha = -0.10$ is used. Aside from the disagreement at 1.025, which is due either to inadequate data or to the use of a dispersion function that is too large for large values of $R_E - R$, this last dispersion function is thus seen to be a reasonable representation of the true dispersion function D_r for ratios not greatly different from unity. As the ratios increase the variation in α becomes important. The integral relation

$$\int_1^{R_I} dR_I P_I(R_I) = \int_1^{R} dR\ P(R) \qquad (4)$$

is in general more convenient than Eqn. (3) for evaluating $\frac{w_L}{w_H}$. Eqn. (4) relates R and R_I for the same fission event.

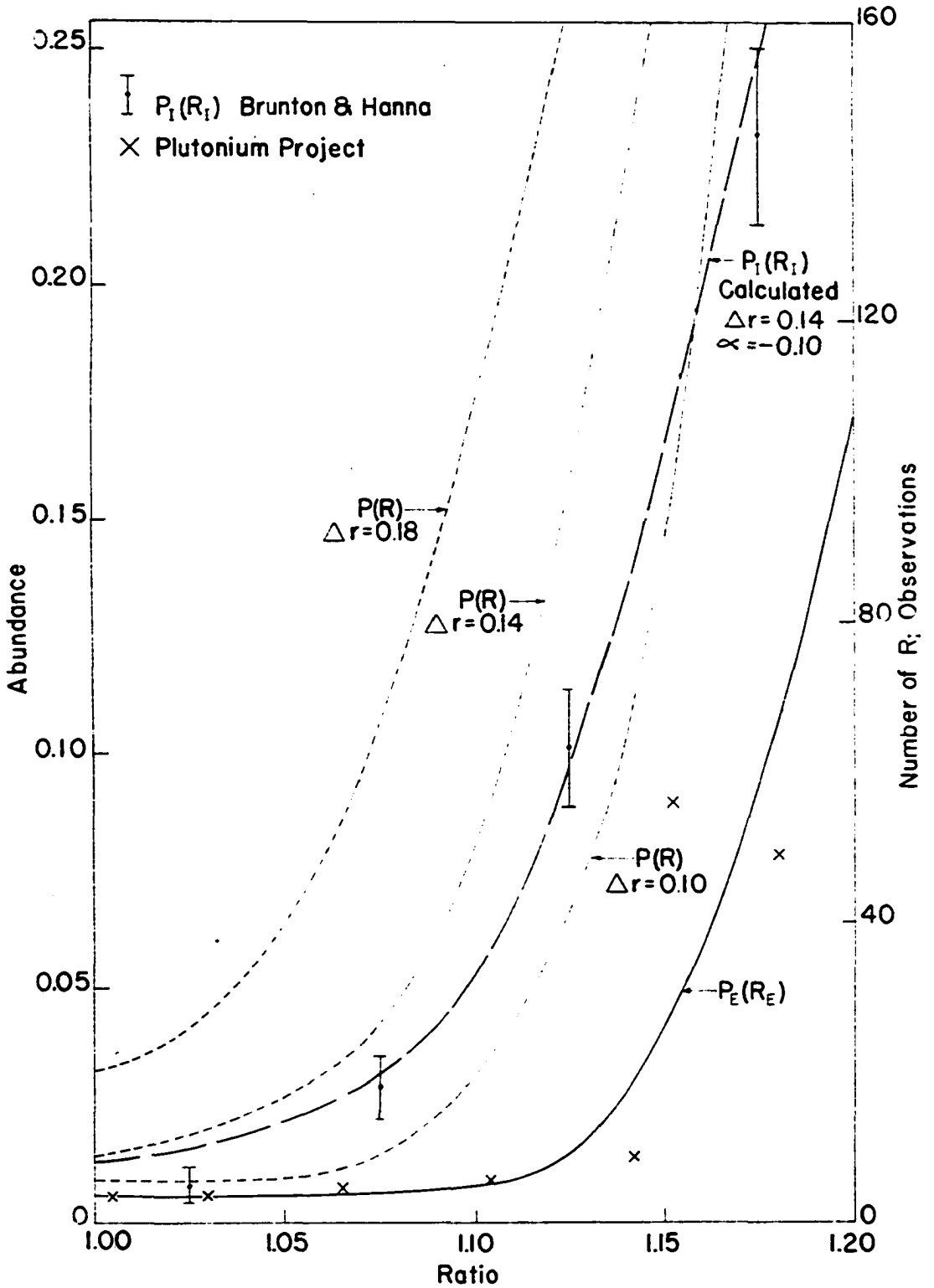

Fig. 2. Comparison of P(R) distributions obtained from trial D_r dispersions.

Since $\frac{w_L}{w_H}$ is the quotient of R and R_I, its dependence on R_I can be found if Eqn. (4) is satisfied.

Application

Not only should the shape and width of the dispersion function D_r be considered, but also its R_E dependence. In practice it is not feasible to determine all by the analytical method. Instead, experimental dispersion data are used to assign an approximate shape and limits of R_E dependence, and then the width is determined by the analytical method. This width determination seems more accurate than a width assigned from present experimental dispersion data alone.

Experimental data on instrumental errors and recoil are in the form of energy dispersions for each fragment. From these the required ratio dispersion can be found. We define the deviations as:

$$e_L = w_L I_L - E_L$$

$$e_H = w_H I_H - E_H$$

$$e = W - E$$

$$r = R - R_E \ .$$

Fig. 3 illustrates the disperison functions such as might arise from variations in the energy deviations e_L and e_H.

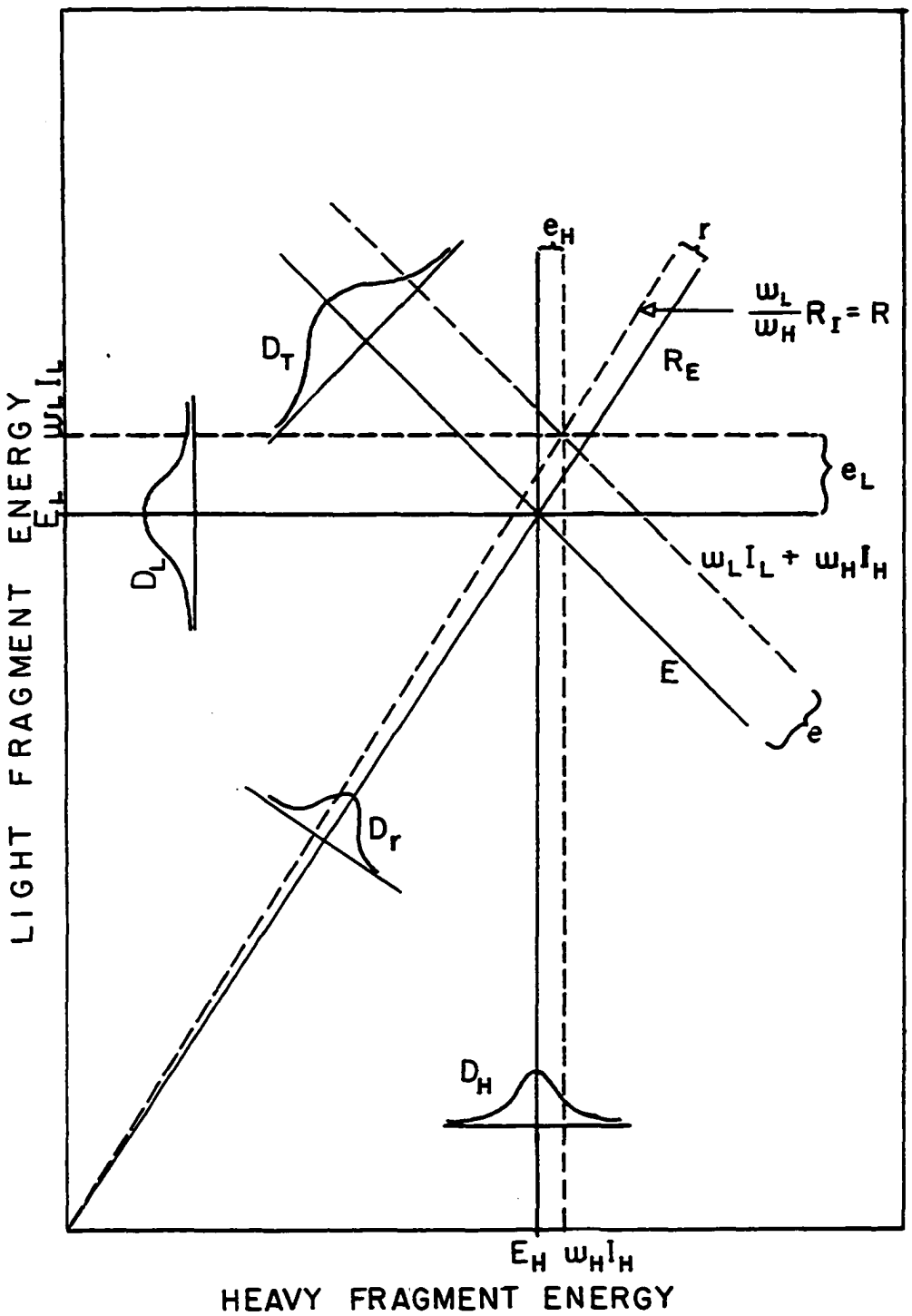

Fig. 3. Energies of a fission fragment pair. The addition of energy deviations to initial energies giving ionization energies is illustrated.

The transformation

$$D_r(R_E,\bar{E};r) = \int_{-E}^{\infty} de\,|J|\,D_L(R_E,\bar{E};e_L)D_H(R_E,\bar{E};e_H) \qquad (5)$$

provides the ratio dispersion from the normalized energy dispersion functions D_L and D_H, where J is the Jacobian $J(\frac{e_L,e_H}{e,r})$. The total energy dispersion D_T is similarily found by

$$D_T(R_E,\bar{E};e) = \int_{-R_E}^{\infty} dr\,|J|\,D_L(R_E,\bar{E};e_L)D_H(R_H,\bar{E};e_H). \qquad (6)$$

It contributes a part of the observed distribution in the total ionization I.

Momentum considerations and the data on neutrons emitted by fragments give information on the neutron recoil contribution to the dispersion. In the extreme cases of forward and backward neutron emission, the fragment recoil energies in the laboratory system are approximately $\pm 2\sqrt{\frac{R_E E\, E_n m_n}{m_L+m_H}}$ for the light fragment and $\pm 2\sqrt{\frac{E\, E_n m_n}{R_E(m_L+m_H)}}$ for the heavy fragment, where E_n and m_n are the neutron energy and mass, respectively. The average values $E_n \cong 2$ Mev[12] and $E \cong 161.1$ Mev give these recoil energies as $\pm 2.4\sqrt{R_E}$ Mev and $\pm 2.4\sqrt{1/R_E}$ Mev, respectively. However, some emitted neutrons have been observed[17] with energies up to 10 Mev in the laboratory system. Since a

---

[17] W. Bothe and W. Gentner, Zeits. f. Physik 119, 568 (1942).

neutron with only the velocity of a fragment has an energy of around 0.7 Mev, it appears that the recoil energy dispersion trails off to energies large compared to its average energy. The symmetry of this dispersion function is determined by the angular dependence on the number and energy of the fission neutrons. For simplicity, the theory of isotropic emission of neutrons from the moving fragments is assumed, giving an essentially symmetric dispersion. Although Peierls[18] has shown an anomaly arising from the isotropic emission theory, two experiments on fission neutrons[12,14] have yielded results consistent with it.

The techniques used in the "back-to-back" double ionization chamber measurements give rise to appreciable instrumental errors. The larger of the reported instrumental deviations and their dispersion widths reported for the two experiments considered[19] are included in Table I.

---

[18] R. Peierls, British Declassified Document B-103.

[19] Two other double ionization chamber measurements on U^{235} slow neutron fission have similar results but are not included. W. Jentschke (Zeits. f. Physik 120, 165 (1943)) had poorer statistics. A. Flammersfeld, P. Jensen, and W. Gentner (Zeits. f. Physik 120, 450 (1943)) used nitrogen as the ionization chamber gas.

Table I. Double Ionization Chamber Fission Data.

	Brunton & Hanna	Deutsch & Ramsey
Number of Fissions	$1.2(10^4)$	$1.7(10^3)$
Ionization Chamber Gas	A plus 3% CO_2	A plus 2% CO_2
Bombardment "Noise" in Chamber	0.45 Mev	1.5 Mev
Energy Loss in U Foil	0.75 Mev	-------
Energy Loss in Collimator	1.25 Mev	-------
Breadth of Channel Analyzer	5 Mev	(Recorded by film)
Drift of Amplifier & Oscilloscope Sensitivity	-------	<2.2 Mev

The combined instrumental dispersion function is not known, but because of the nature of the deviations the function is probably symmetric.

Since the deviations are much smaller than the fragment energies of around 80 Mev, it is sufficiently accurate to use the expanded form $r \cong \frac{e_L - R_E e_H}{E_H}$, which gives a linear transformation. It is also allowable to use infinite limits of integration so that Eqns. (5) and (6) reduce to

$$D_r \sim \int_{-\infty}^{\infty} de\ D_L\ D_H \tag{7}$$

$$D_T \sim \int_{-\infty}^{\infty} dr\ D_L\ D_H. \tag{8}$$

In order to make a trial calculation, the combined dispersions in energy, D_L and D_H, are assumed to be the Gaussian

functions

$$D_L \sim \exp\left[\frac{-2.8\ e_L^2}{(\Delta e_L)^2}\right]$$

$$D_H \sim \exp\left[\frac{-2.8\ e_H^2}{(\Delta e_H)^2}\right],$$

where Δe_L and Δe_H are the full widths of the dispersions at half maximum.

The R_E dependence of $\Delta e_L(R_E,E)$ and $\Delta e_H(R_E,E)$ is uncertain, but the extremes of dependence are found by assuming the recoil dispersion negligable or the instrumental dispersion negligable. For the first case $\Delta e_L = \Delta e_H = \Delta e_S$, where Δe_S is the symmetrical fission dispersion width; for the second case, on the assumption that E_n is independent of R_E, we have

$$\Delta e_L = \sqrt{R_E}\,\Delta e_S$$

$$\Delta e_H = \frac{\Delta e_S}{\sqrt{R_E}} .$$

Substitution of the assumed Gaussian energy dispersions with these widths in Eqn. (7) gives a Gaussian ratio dispersion D_r whose width, for the first case, is

$$\Delta r = \frac{\Delta e_S \sqrt{R_E^2 + 1}\,(R_E + 1)}{\overline{E}} \quad ; \qquad (9)$$

and, for the second case, is

$$\Delta r = \frac{\Delta e_S \sqrt{2R_E\,(R_E+1)}}{\bar{E}} \quad . \tag{10}$$

In the graphical analysis to be performed, however, these extremes give results that differ insignificantly, so the uncertainty in R_E dependence is unimportant.

The nature of the $\bar{E}$ dependence of D_r is shown by Eqns. (9) and (10). The small variation of an average E with fission asymmetry is seen[9,15] from $P_I(R_I,I)$ by using an approximate value of w. The width of the distribution in E about average E is roughly only 13 percent of average E. Thus, this average E should be near the $\bar{E}$ required by Eqn. (2).

Since neither $P_E(R_E)$ nor $P_I(R_I)$ have simple mathematical representations, P(R) is found by approximating $P_E(R_E)$ by a step function and dispersing the amplitude of each step to other steps. Three such P(R) distributions obtained from Gaussian ratio dispersions of symmetric fission Δr widths 0.10, 0.14, and 0.18 are illustrated in the region of symmetrical fission by Fig. 2. The most suitable width of 0.14 when varied within the limits of Eqns. (9) and (10) gives the P(R) distribution shown in Fig. 1.

The $\frac{w_L}{w_H}$ variation is found by solving Eqn. (4) by graphically integrating the distributions in Fig. 1.

Since Δr is small the integral relation (4) can be extended to

$$\int_1^{R_E} dR_E \; P_E(R_E) \cong \int_1^{R_I} dR_I \; P_I(R_I) = \int_1^{R} dR \; P(R),$$

and a value of integrated abundance in Fig. 4 represents approximately the same fission event for the three ratios. The approximate $\frac{W_L}{W_H}$ dependence on R_E or R_I shown in Fig. 5 is obtained by comparing R with R_I. In view of the rather arbitrary selection of dispersion function, the results are to be considered as only an estimate. When substituted in Eqn. (3), the $\frac{W_L}{W_H}$ variation of Fig. 5 and the P(R) distribution in Fig. 1 give a $P_I(R_I)$. This serves as a check on the accuracy of the dispersing and integrating calculations.

Results

According to Bohr[16] the energy lost through nuclear collisions in stopping fission fragments is appreciable at low velocities in comparison with electronic collision energy loss. In order to compare the results in Fig. 5 to this theory we assume that the parts E_L and E_H of nuclear collision energy losses not producing ionization

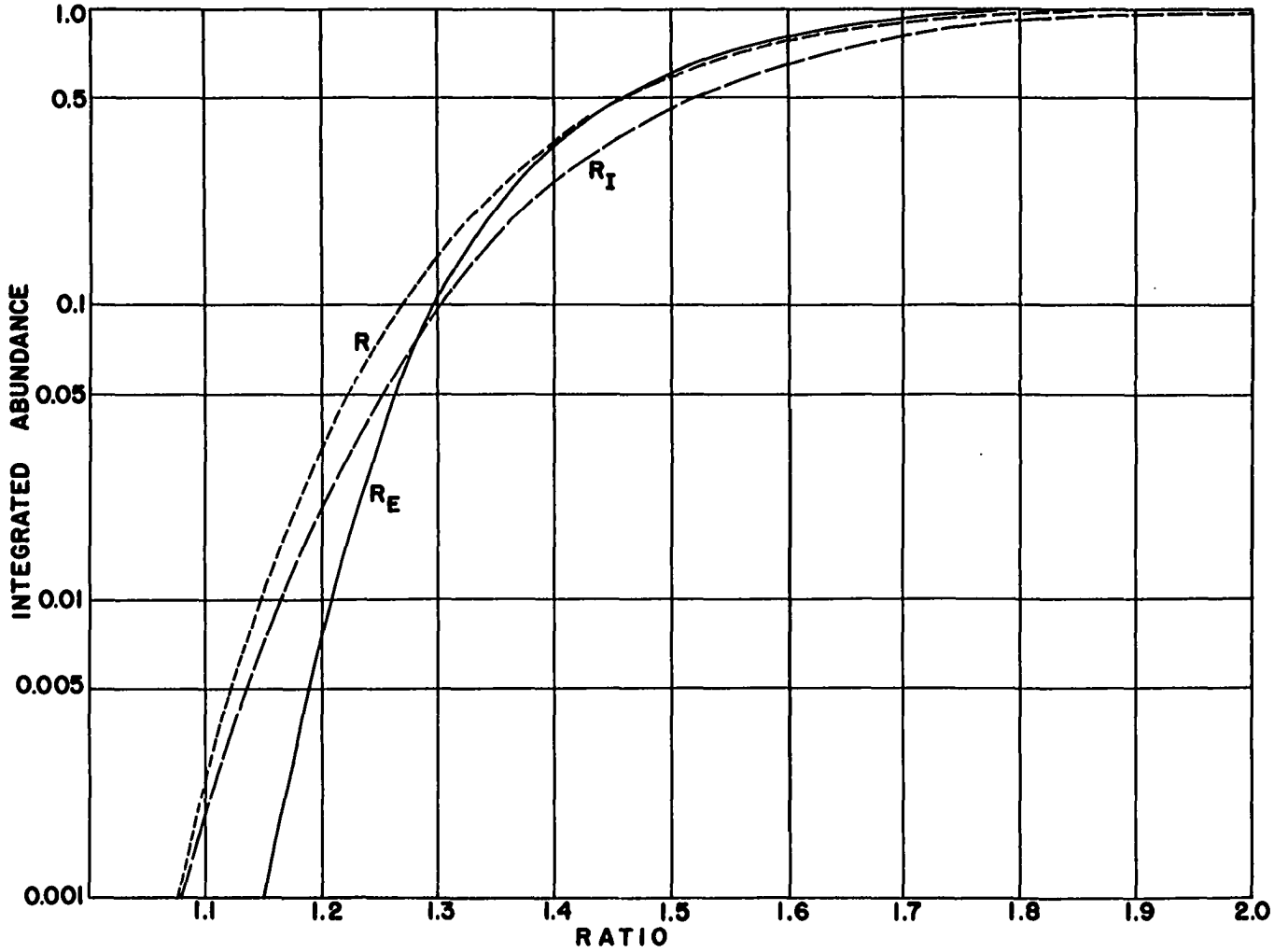

Fig. 4. Integration curves of ratio distributions.

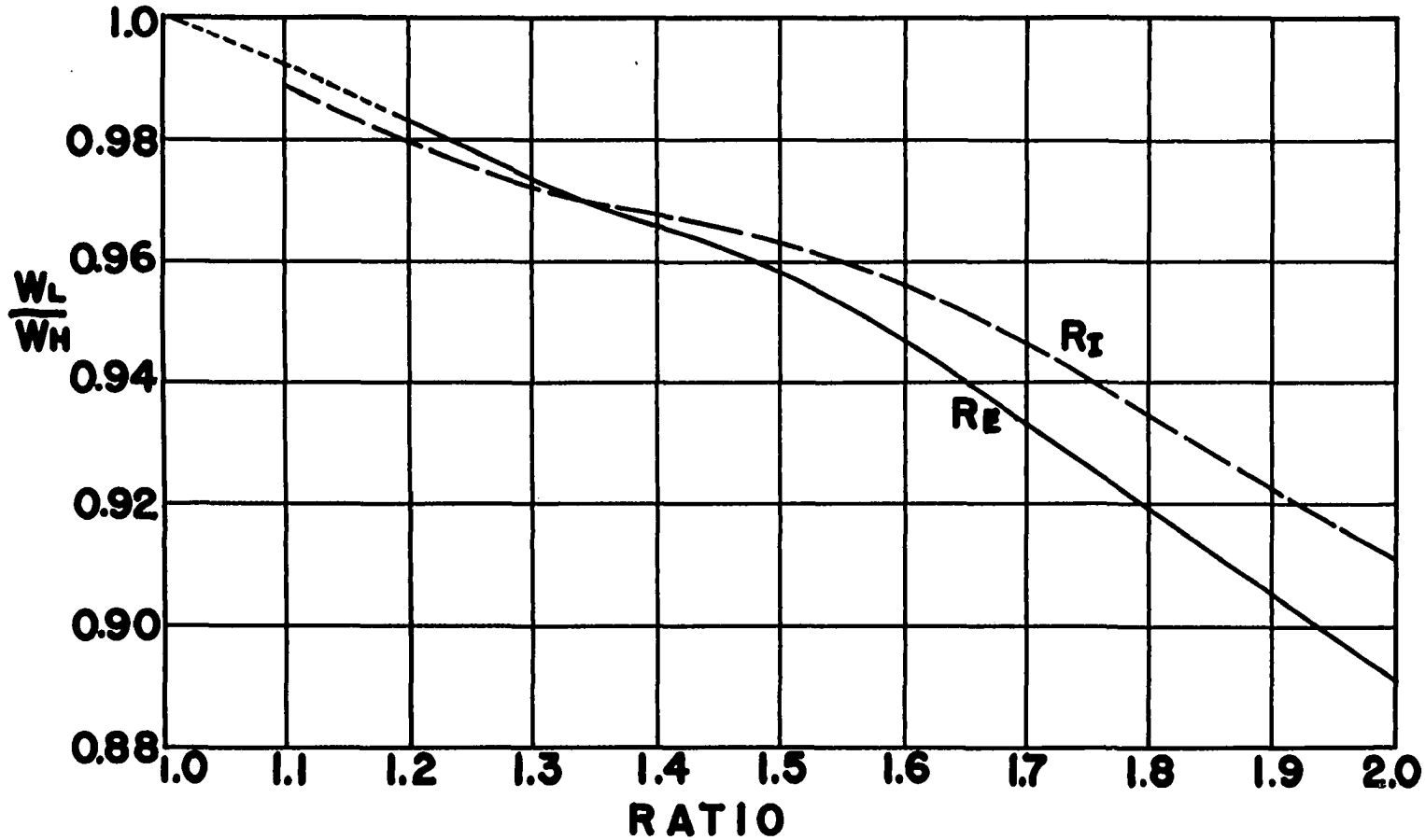

Fig. 5. The approximate dependence of w_I/w_H upon fission asymmetry.

are related by

$$\frac{E_L^N}{E_H^N} = \frac{m_L v_L^2}{m_H v_H^2} ,$$

where the velocities v_L and v_H are the critical velocities at which the nuclear collision and electronic collision energy loss rates are equal. Using the velocity expression given by Knipp[20] we have

$$\frac{v_L}{v_H} = \left[\frac{Z_L^{4/3} m_H}{Z_H^{4/3} m_L}\right]^{1/3} ,$$

where Z is the nuclear charge.

If the rest of the energy is lost with the energy/ionization ratio w_e, then the ionization energies are

$$w_L I_L = w_e I_L + E_L^N$$

$$w_H I_H = w_e I_H + E_H^N ,$$

from which it follows that

$$\frac{w_L}{w_H} = \frac{1 + \frac{E_L^N}{I_L w_e}}{1 + \frac{E_H^N}{I_H w_e}} . \qquad (11)$$

---

[20] J. K. Knipp, Bull. Am. Phys. Soc. 25, 6 (1950).

Comparison of Fig. 5 and Eqn. (11) gives 3.4 Mev for E_H^N and 1.9 Mev for E_L^N for the most probable fission ratio. On this basis, about 5.3 Mev is not observed as ionization and should be added to reported energy value of 155.8 Mev[15] to give an average total kinetic energy value of 161.1 Mev. This is in good agreement with the estimate given by Henderson[7] of 165 ±8 Mev.

Evaluation of the dispersion width found analytically gives Δe_S = 8.1 Mev, a value confirmed by the instrumental error and recoil data. The total energy dispersion width as found from Eqn. (8) is a sizeable part of the observed[11] distribution in I for fission of greatest asymmetry, but a very small part for nearly symmetrical fission as seen in Table II. Although not fully understood the rest of the

Table II. Comparison of Dispersion and I Distribution.

R_I	Width of I Distribution in Mev	Δe in Mev.
1.2	30	11.5
1.5	18	11.8
2.0	15	12.5

distribution width in I is probably to be attributed to variations in the β-, γ-, and neutrino-radiation energies and to variations in fragment nuclear charge.

The method of analysis presented here is limited in usefulness primarily by scant data on the dispersion function. The distribution $P_I(R_I)$ has been confirmed by several experiments and has good statistics. Since most of the points on the Plutonium Project U^{235} fission mass yield curve have a precision of about five percent,[21] such errors would account for only a small part of the difference between $P_E(R_E)$ and $P_I(R_I)$.

It should be noted that a variation in the number of neutrons per fragment results in a $P_E(R_E)$ distribution different from the distribution in $\frac{m_H}{m_L}$. The effect of such a variation is to disperse $P_E(R_E)$ into the $\frac{m_H}{m_L}$ distribution in much the same manner that the energy dispersion disperses $P_E(R_E)$ into $P(R)$. The magnitude of this neutron number dispersion is much smaller; for example, a distribution width of 1/2 in the number of neutrons per fragment leads to a ratio dispersion width of about 0.01, which is much smaller than the ratio dispersion arising from energy deviations. Any correction for this neutron number variation would be to narrow the distribution $P_E(R_E)$ and its principal effect would be an insignificant broadning of D_r.

---

[21] M. S. Freedman and E. P. Steinberg, CC 3420.

RANGE-IONIZATION APPARATUS

Corson and Wilson[22] have derived the voltage equation for electron collection between parallel plates of separation ℓ. They found the electron collection voltage V_c at time t after the ionizing event can be expressed by

$$V_c = \frac{V}{\ell C} \int_0^t \int_0^{\ell - vt} \sigma(x)dx\, dt, \qquad (12)$$

where C is the capacity of the collector electrode to ground, v is the constant drift velocity of electrons, and the charge density $\sigma(x)dx$ is the number of electrons formed between the perpendicular distances x and $x+dx$. Since the fragment tracks are straight and originate at the negative electrode, a range measurement r along a track is linearly related to the perpendicular distance x by $r \cos\theta = \ell - x$, where θ is the angle between x and r.

The experimental arrangement is schematically shown in Fig. 6. Details of the equipment are discussed in this section. The purpose of the differentiating circuit is to provide a waveform of the time variation of dV_c/dt for oscilloscope presentation. Such a waveform is interpreted as range-ionization data as shown in the Fig. 7 sketch. The residual ionization multiplied by w_e gives the fragment

---

[22] D. R. Corson and R. R. Wilson, Rev. Sci. Inst. 19, 207 (1948).

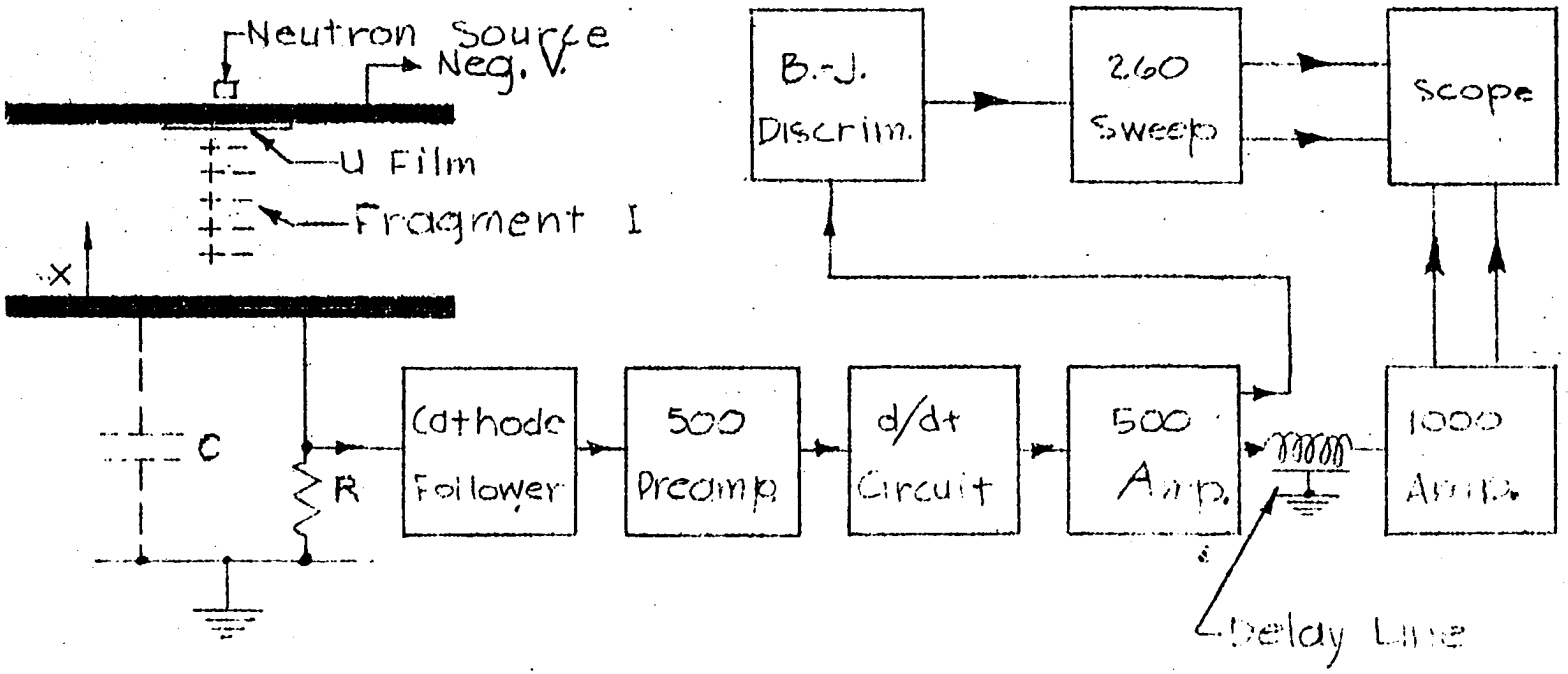

Fig. 6. Schematic diagram of the electron collection equipment with a single ionization chamber.

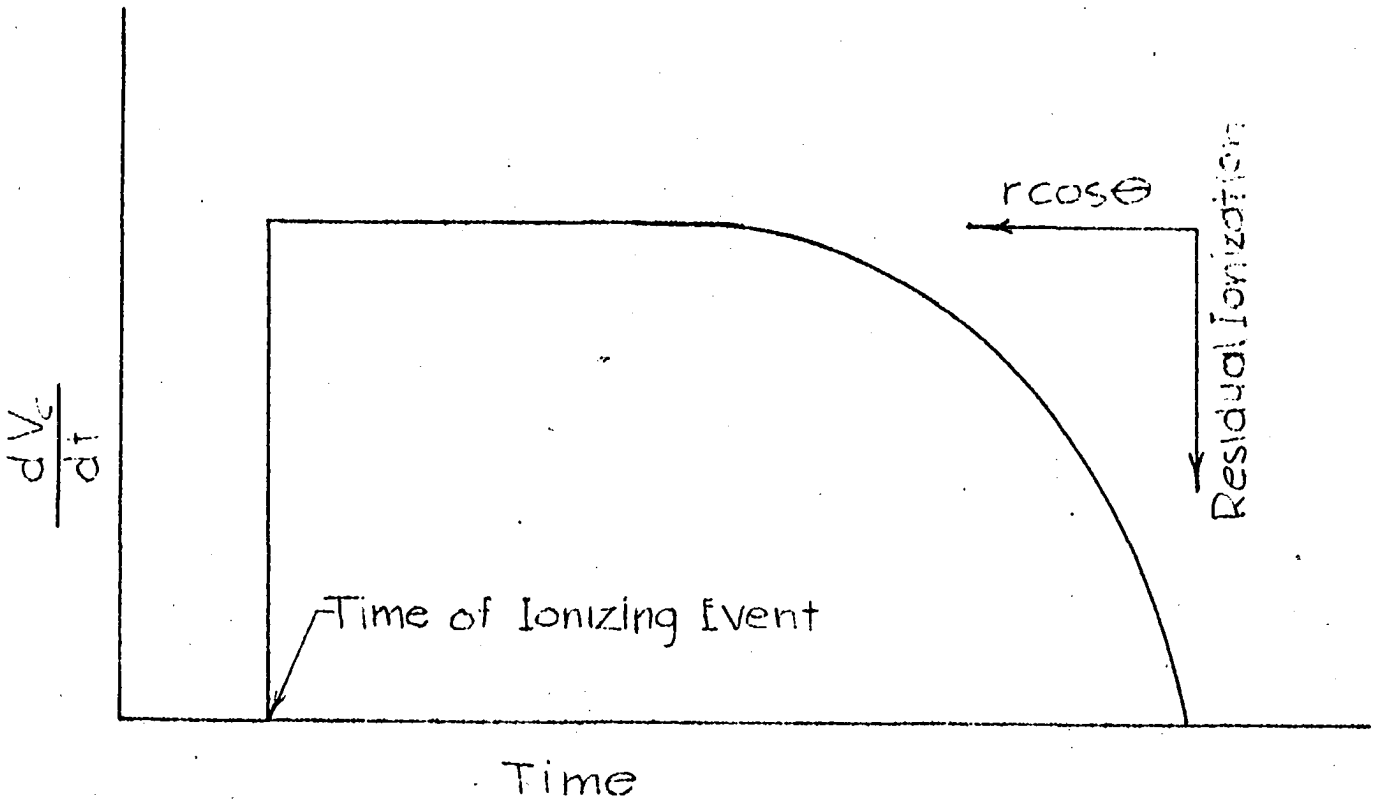

Fig. 7. Sketch of the oscilloscope waveform showing coordinates of the range-ionization data.

kinetic energy minus the unobserved energy to be lost in nuclear collisions. In this manner the equipment to be described provides range-ionization data, from which can be obtained range-energy information.

Ionization Chamber

The ionization chamber shown in Fig. 8 was a 7-in. long, 6 3/4-in. I. D. brass tube, to which was silver soldered an end plate containing a compound pressure gauge. The base plate was grooved to match the brass tube. Four machine bolts between the two end plates and a Teflon gasket in the groove were used to make the chamber gas tight.

A gas purifier was installed to remove oxygen gas from the chamber. Oxygen forms heavy negative ions of low mobility, the formation of which would cause deviations from the desired V_c as expressed by Eqn. (12). Attached to the chamber by 1/4-in. tubular Kovar glass-to-metal seals, the purifier circulates the gas by convection through copper filings maintained at 400°C by an electrical heater. Calcium metal at 250°C was used for purification of argon during some readings. A container of anhydrone (magnesium perchlorate) similarly attached to the chamber removed water vapor, which also forms negative ions. The chamber was evacuated by a Cenco Hyvac pump to 10-50 μHg as read on a McLeod gauge and filled with gas from standard tanks

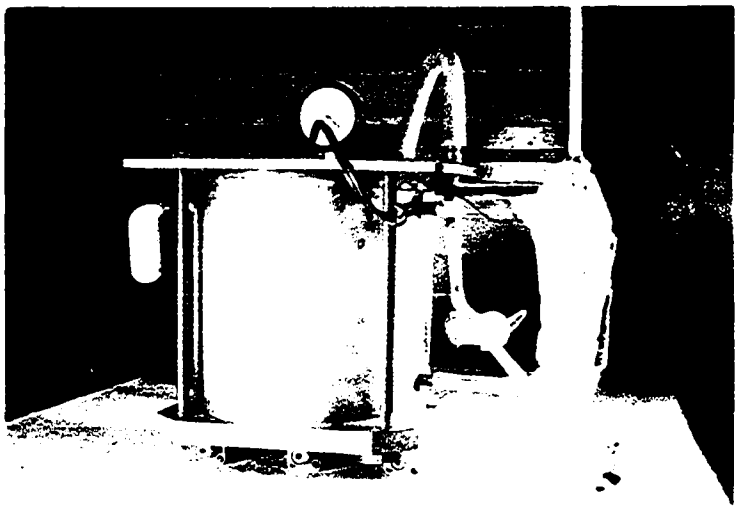

Fig. 8. Exterior of the ionization chamber showing the gas purifier on the right and electrical connections at the bottom.

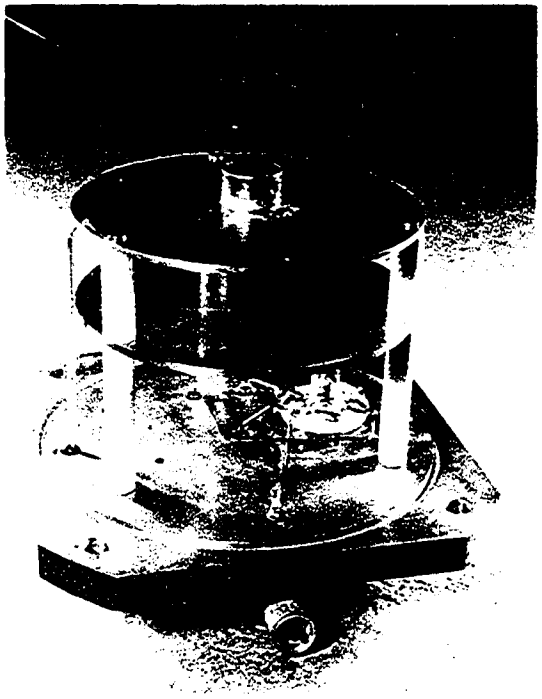

Fig. 9. Interior of the single ionization chamber showing neutron source holder on the upper electrode.

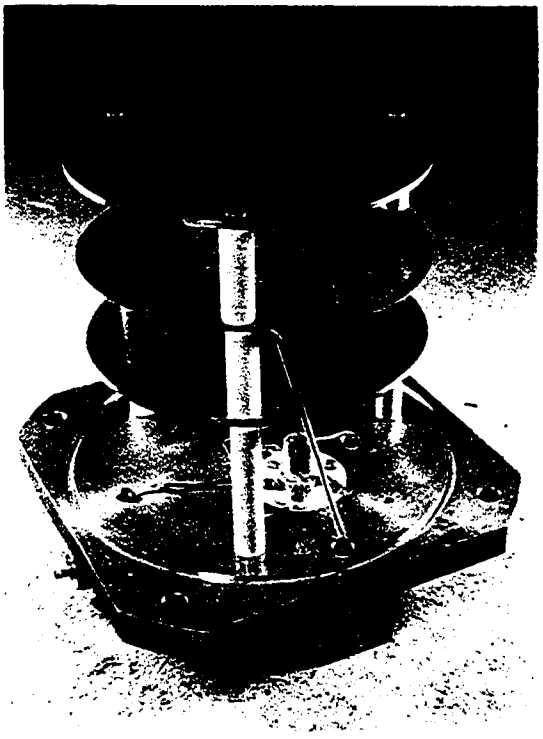

Fig. 10. Interior of double ionization chamber. The screen support for the source is in the center.

to pressures as indicated by the chamber gauge. The chamber was closed off by a stopcock during readings.

Figs. 9 and 10 show the electrodes and their mounting on the base plate for the single and double chambers, respectively. Except for the high voltage electrode of the double chamber experiment, the electrodes were 1/8-in. brass plates 5 3/4 in. in diameter supported by 1/2-in. diameter ceramic insulators. Electrical connections into the chamber were by insulated Kovar terminals. Inside the chamber, wires requiring insulation were enclosed in glass tubes. The only circuit components placed inside the chamber were vacuum tubes and glass enclosed resistors. This type of construction in the interior of the chamber minimized the use of organic materials which emit contaminating gasses.

The negative voltage source for the high voltage electrode was a battery supply in a shielded box connected by a shielded cable to the chamber. A simple resistance and capacity filter was used at the batteries to reduce high frequency pick-up.

The thin film of uranium used in the single chamber experiments was made by a dipping method. The high voltage electrode plate was ground to a plane surface by successively finer abrasives and then given a mirror finish on a rouge wheel. The finished surface was given four dips in a uranium nitrate-Zapon solution containing 45 g of Zapon

and 307 g of Zapon thinner in which had been dissolved 12 g of uranium nitrate (natural uranium). The plate was placed in a vertical plane to drain in a different direction after each dip and then allowed to dry. The plate was washed with Zapon thinner and alcohol so as to leave a central 2-in. diameter filmed area. By heating the plate for about one hour at 460°C the organic material was driven off and the uranium nitrate was changed to U_3O_8. As determined by alpha activity, the uranium content of the film was 76 $\mu g/cm^2$.

A Po-Be source having an activity of about $5(10^4)$ neutrons per second during the readings was placed inside the chamber on the upper side of the high voltage electrode plate. Even with this rather thick film and favorable geometry the fission rate was only eight per hour.

Electronic Equipment

An important factor in the quality of the data is the signal/noise ratio obtained for the fission fragment dV_c/dt signal. For a given number of ion pairs and collection time, V_c in Eqn. (12) is increased only by reducing C. In order to minimize the capacitive loading on the collecting electrode, a cathode follower employing a 955 tube was used inside the chamber. The 104-megohm

Victoreen resistances R was inside the chamber, but the 2.2K cathode resistance and the filter for the 100-volt plate supply were outside the chamber in the terminal shield. The filament was battery heated. The value of C was 17 $\mu\mu$f with the cathode follower in use, whereas C was 37 $\mu\mu$f when the collecting electrode was instead connected through standard connectors to the input of the preamplifier.

As is pointed out by Corson and Wilson,[22] noise is principally due to Johnson effect from the input resistor and to shot effect in the first tubes. The mean square voltage due to the Johnson effect in a resistor R across a capacity is

$$V_J^2 = \frac{2KT}{\pi C} \tan^{-1}\left[\frac{2\pi RC(f_2-f_1)}{1+4\pi^2 R^2 C^2 f_1 f_2}\right] , \qquad (13)$$

where K is Boltzmann's constant, T is temperature, and f_1 and f_2 are the lower and upper cut-off frequencies of the amplifier. Since the practical lower limit of the product RC is determined by the pulse length, V_J is minimized by the use of large values for R. With the choice of R =104 megohms the RC decay time was small compared with the time between alpha- or fission fragment ionizations in the chamber so there was negligable time overlap of signals. Due to the low output impedance of the cathode follower, Johnson noise

from the input resistance of the preamplifier was negligable. The shot effect noise, usually of the order of 10 microvolts r.m.s., was increased by about $\sqrt{2}$ by the use of the cathode follower. Shielded cables and chassis were used, but largely because of pick-up the total noise was about 40 microvolts r.m.s.

In order that the amplification be true, the electron collection time of the chamber must be large compared with the response time of the amplifier. In particular, it must be large compared with the response time of the waveform trailing edge, which is of interest. The preamplifier and main amplifier used in this experiment were modifications of the Los Alamos Model 500 amplifier,[23] which has a rise time of about 0.1 μsec. for a test pulse. After modifications the fall time was 0.15 μsec. for a test pulse. The negative high voltage for the chamber was then chosen to give collection times of about 10 μsec.

In order to pass a 10-μsec. pulse, the interstage time constants of amplifier and preamplifier were increased to 220 μsec. The decreased fall time was obtained by reversing the polarity of the signal in the last stages of amplification so that the output pulse was negative. This

---

[23] W. C. Elmore and M. Sands, Electronics (McGraw-Hill Book Company, Inc., New York, 1949).

required changes in the biases of these tubes. As a result of this modification, the output cathode follower of the amplifier had its lowest output impedance during the trailing edge, a positively rising waveform.

Differentiation of the V_c waveform was by the circuit shown in Fig. 11. The circuit performed the operation

$$\frac{\Delta V_c}{\Delta t} = \frac{V_c(t) - V_c(t-\Delta t)}{\Delta t} \quad , \qquad (14)$$

where the delay time Δt was chosen as 0.4 μsec. to be small compared with the electron collection time. With these conditions the accuracy of differentiation was good. A detailed treatment of differentiation error is in the Discussion section.

The differentiator circuit provides a negative, time retarded signal $-V_c(t-\Delta t)$ and adds it to the signal V_c. Positive and negative V_c signals are provided by the paraphase amplifier T_1, the negative signal of which is delayed by the delay line (General Electric continuous type) in T_2. Unbalances in the circuit and attenuation of delay line are compensated by the positive signal amplitude adjustment in the cathode of T_1. Addition is performed by T_3 and T_4. The cathode follower T_5 presents a high impedance to the adding network and a low impedance output. The factor Δt in Eqn. (14) and the non-unity gains of the tubes combine as a constant scale factor.

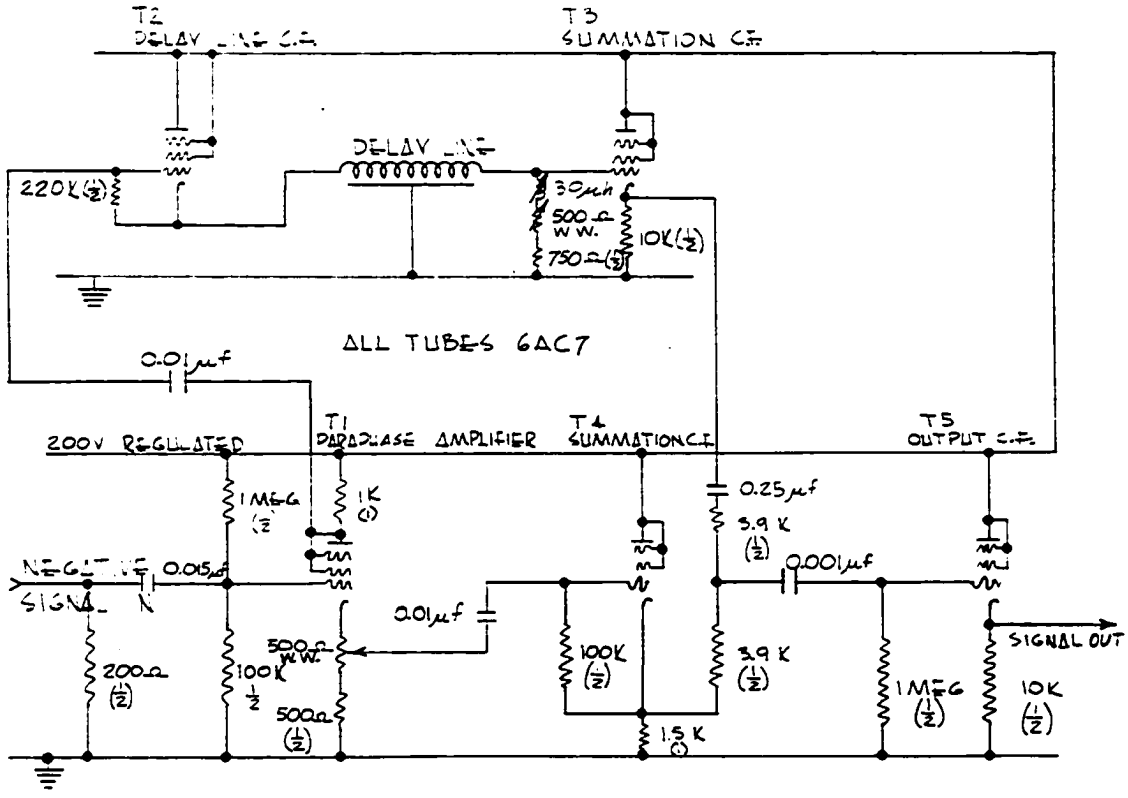

Fig. 11. Differentiator Circuit.

The Frisch method of shorted delay line differentiation is simpler than the circuit used, but has the disadvantage that accurate compensation for the delay line attenuation is not possible. The error due to an uncompensated delay line attenuation would be appreciable for $\Delta t = 0.4\ \mu$sec. or larger.

The differentiated signal from the Model 500 amplifier was delayed by 0.8 μsec. in order to display its beginning on the driven sweep of the oscilloscope. The additional use of a Los Alamos Model 1000 amplifier[23] following the delay line gave needed voltage gain and low impedance, push-pull outputs to the vertical plates of the oscilloscope. Beaded, coaxial cables of low capacity (200-ohm, 5.5- $\mu\mu$f/ft. Transradio cables) were used for the connection.

A Bell-Jordan[24] circuit was used for pulse amplitude discrimination of an undelayed signal from the Model 500 amplifier. With the discriminater bias set just above the level of alpha-pulses, sweep triggers were generated for all fission fragment pulses and for occasional alpha-pulses that had combined with noise. Driven, linear sweeps were provided by a Los Alamos Model 260 sweep generator,[23] the output tubes of which were duplicated to provide simultaneous sweeps for the dual-beam oscilloscope.

---

[24] W. Jordan and P. Bell, Rev. Sci. Inst. 18, 703 (1947).

The use of a DuMont type 5SP11 cathode ray tube allowed simultaneous display of the two fragments on two beams. A single sweep was used for observations with one chamber. An overall acceleration of 8000 volts from radio frequency power supplies[23] gave a bright oscilloscope trace for photography of fast sweeps. Eastman Linograph Ortho or Super-XX film were used at f/4 or f/3.5, respectively, in a DuMont 271-A camera for oscilloscope photography. With a blue filter over the oscilloscope tube face and the camera shutter open, oscilloscope pictures with satisfactory contrast and background were taken with a film speed of 1 ft./hr.

Fig. 12 is a photograph of the entire apparatus as used for the single chamber experiment.

Double Chamber Equipment

The simultaneous observation of range-ionization by the electron collection method required a duplication of differentiator and amplifier equipment and the use of a uranium film on a thin backing between two collecting plates. In the double chamber arrangement shown in Fig. 10 the neutron source was placed on the upper collecting plate 4 cm from the uranium film. This poorer neutron geometry meant that excessively long observations would be required to obtain a large quantity of data from films of desired

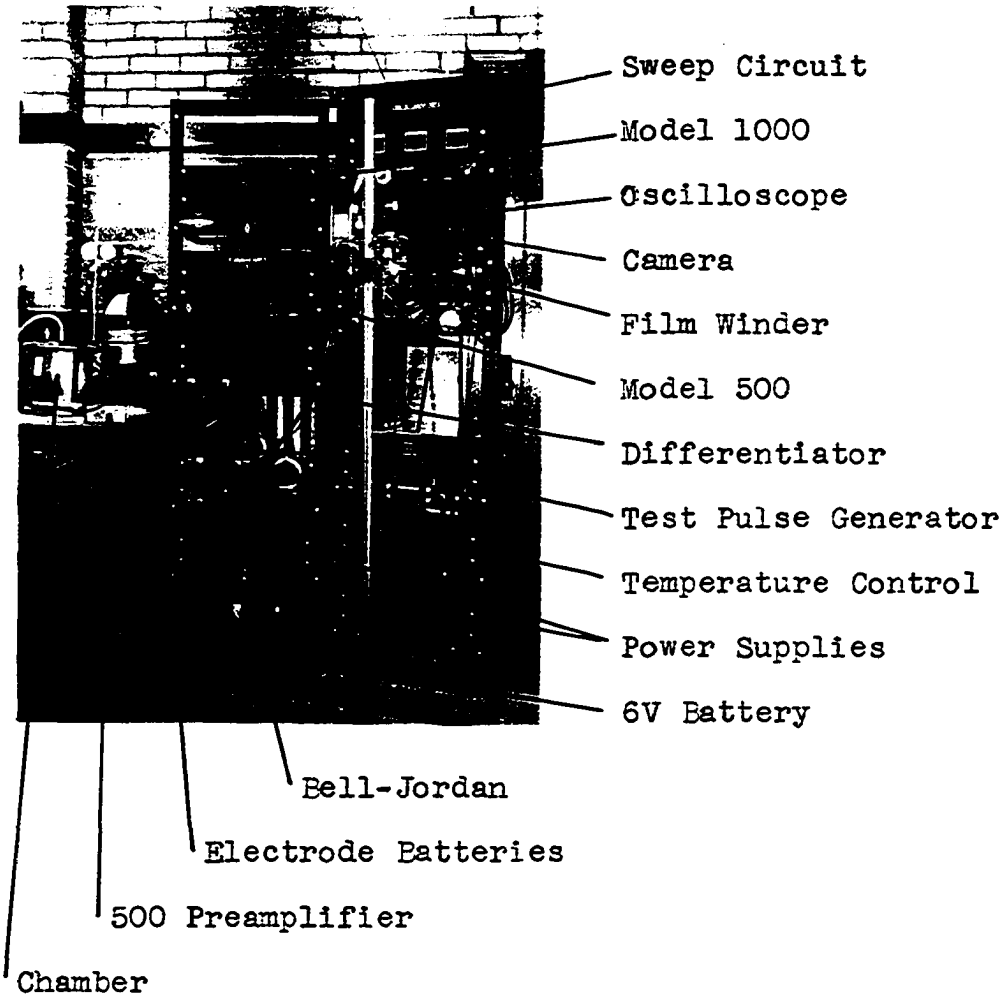

Fig. 12. Photograph of the single ionization chamber and associated electronic equipment. Although not visible, the outputs of the Model 1000 amplifier are only a few inches from the oscilloscope inputs.

thickness. Consequently, a thicker film was used and relatively few observations were made.

Copper window screen was used as a support for a thin Zapon film, on one side of which had been sprayed uranium nitrate (natural uranium). The screen was held between two circular, thin metal sheets in which 2-in. holes had been centered. To make the Zapon film a glass plate was dipped twice in a 10 percent Zapon solution and the film was removed in distilled water. The film was about 30 $\mu g/cm^2$. A metal ring painted with Glyptol was placed on the floating film. This film, held by the ring, was sprayed with a solution of uranium nitrate in ethyl alcohol (40 mg per ml) by a small atomizer. It was found necessary to paint the Glyptol seal with Formvar to prevent softening by alcohol. A fairly uniform uranium deposit was obtained by allowing drying periods between several sprayings. The uranium content of the film as measured by alpha-activity was 160 $\mu g/cm^2$. This film in the double chamber arrangement gave a fission rate of about one per hour.

A duplicate of the cathode follower inside the chamber (except for substitution of the 104-megohm resistor by a 31-megohm resistor) was connected to the upper collector electrode. The signal from this upper plate was amplified by the Model 500 and Model 1000 amplifiers and used to trigger the sweep circuit in the same manner as in the

single chamber experiment. Although some fragments were lost to the supporting screen, mounting the Zapon film below the screen insured that sweep presentations of fission were always of pairs. The uranium was on the upper surface of the Zapon film.

The lower collector electrode was connected through the other cathode follower to a Los Alamos Model 100 preamplifier,[23] the output of which was differentiated by a duplicate of the differentiator circuit. After going through a 0.4-μsec. delay line the signal was further amplified in the Model 100 amplifier and used to deflect the beam of the second sweep. By using beaded, coaxial cable as an output connection to the oscilloscope a trailing edge response time of 0.5 μsec. was obtained. As seen by Eqn. (13) the narrower band pass associated with this slower response time reduces the noise. Although the expedient use of different types of amplifiers on the two chambers resulted in different treatment of the data, it was not considered worthwhile to duplicate the 500-1000 amplifying equipment. The usefulness of the double chamber data was limited by poor statistics rather than amplifier response.

EXPERIMENTAL RESULTS

No accurate data have been reported on either the diffusion of electrons in an ionization chamber or ion recombination in regions of high ion density. These factors especially affect the range-ionization data from electron collection equipment in which relatively long collection times are employed. Although the equipment described in the last section was not ideally suited for measurements of diffusion and recombination, it was used to obtain rather rough data of these factors for various gasses. These data enabled a better understanding of the range-ionization data, which were taken with greater precision and detail.

Recombination and Diffusion Measurements

A fission fragment or alpha-particle stopped in a gas leaves a dense column of ion pairs which tend to recombine by Coulomb attraction. In experiments in which the collection time may be small, pressures and fields giving a high electron agitation velocity are used to spread apart the ions by diffusion before columnar recombination is appreciable. According to Rossi and Staub,[25]

---

[25] B. B. Rossi and H. H. Staub, Ionization Chambers and Counters (McGraw-Hill Book Company, Inc., New York, 1949).

no reliable recombination data are available even for the simpler case of uniformly distributed ionization. However, they state that the time rate of recombination per unit volume is expected to be proportional to the square of the density of ions, where the factor of proportionality seems about the same for different gasses.

For the electron collection experiment, it appears from the above that a choice of gas is a compromise between effects of diffusion and recombination. No gas is expected to have low recombination and diffusion. Recombination lowers V_c and thus the signal/noise ratio. Furthermore, recombination distorts the shape of the range-ionization curve unless, contrary to the above expectation, recombination is proportional to the ion density along the fragment track. On the other hand, diffusion has the effect of a time variation of the charge density σ resulting in a deviation from V_c of Eqn. (12).

The experimental results were in agreement with these expectations. The low fission yield made a fission fragment recombination study impractical, so the study was instead made with the less dense ionization of uranium alpha-particles. The results shown in Fig. 13 are the maximum undifferentiated pulse heights from the 76 $\mu g/cm^2$ uranium source with 3.81-cm electrode separation for different field strengths and gas pressures. Gasses were not

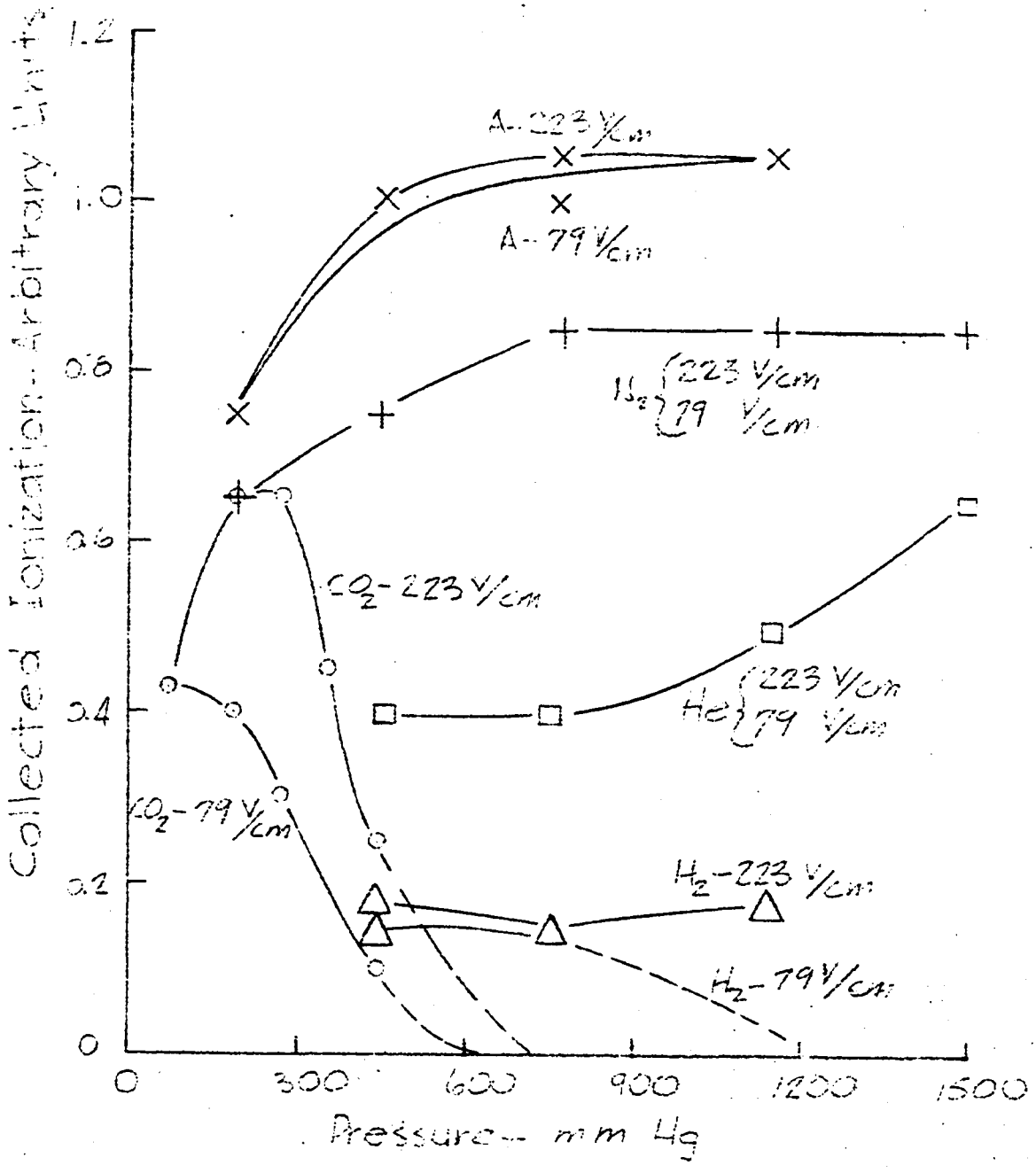

Fig. 13. Effect of recombination on alpha-particle pulse height. Dotted extentions are below the noise level. Decreased pulse heights at low pressures are due to excessive range.

purified in this experiment.

The data compiled in Table III are useful for an

Table III. Experimental w Data and Semi-Emperical Data of Alpha-Particle Range and Electron Agitation Velocity.

Gas	w in ev/ion pair for 5.3-Mev Alpha-Particles	Range in cm at N.T.P.	u in 10^6 cm/sec. for N.T.P. and 760 V/cm
CO_2	34.6	3.8	14
H_2	36.0	16.5	35
N_2	35.6	3.3	53
He	31.0	18.8	84
A	24.9	3.4	195

understanding of the data in Fig. 13. Ranges are calculated for the uranium 4.76-Mev alpha-particle from data compiled by Livingston and Bethe.[26] It should be noted that for low gas pressures, especially in the cases of hydrogen and helium, alpha-particle ranges exceeded chamber dimensions. Also to be noted is that the variation of w with gas contributed to the variation of pulse heights in Fig. 13. The values of w and u are from Rossi and Staub,[25] except that their w value for air is used for nitrogen in the table. Although the experimental data of Fig. 13 had these inaccuracies, they did confirm that

---

[26] M. S. Livingston and H. A. Bethe, Rev. Mod. Phys. 9, 245 (1937).

recombination increases with pressure, i.e. with ion density. Furthermore, when compared with the tabulated values of electron agitation velocity, these data confirmed that electron diffusion decreases recombination.

The demonstration that recombination increased with pressure made it appear that possible range-ionization data distortions due to recombination would be detected by comparing fission fragment data taken at two different pressures. In the fission fragment recombination experiment, the collection time at both pressures was the same both to facilitate comparison of data and to further increase the recombination at the higher pressure because of the lower agitation velocity. This lower agitation velocity is associated with the lower drift velocity required for the smaller electrode separation. In the case of both argon and nitrogen, a comparison of fission fragment range-ionization data taken for one-half and one atmosphere pressure with 7.62-cm and 3.81-cm electrode separation, respectively, indicated no distortion due to recombination. Results for nitrogen and argon are in Figs. 14 and 15, respectively. The normalization of these data is explained in the next subsection.

Except for the use of an 80 percent U^{235} source, the equipment used in the fission fragment recombination experiment was the single chamber equipment described in

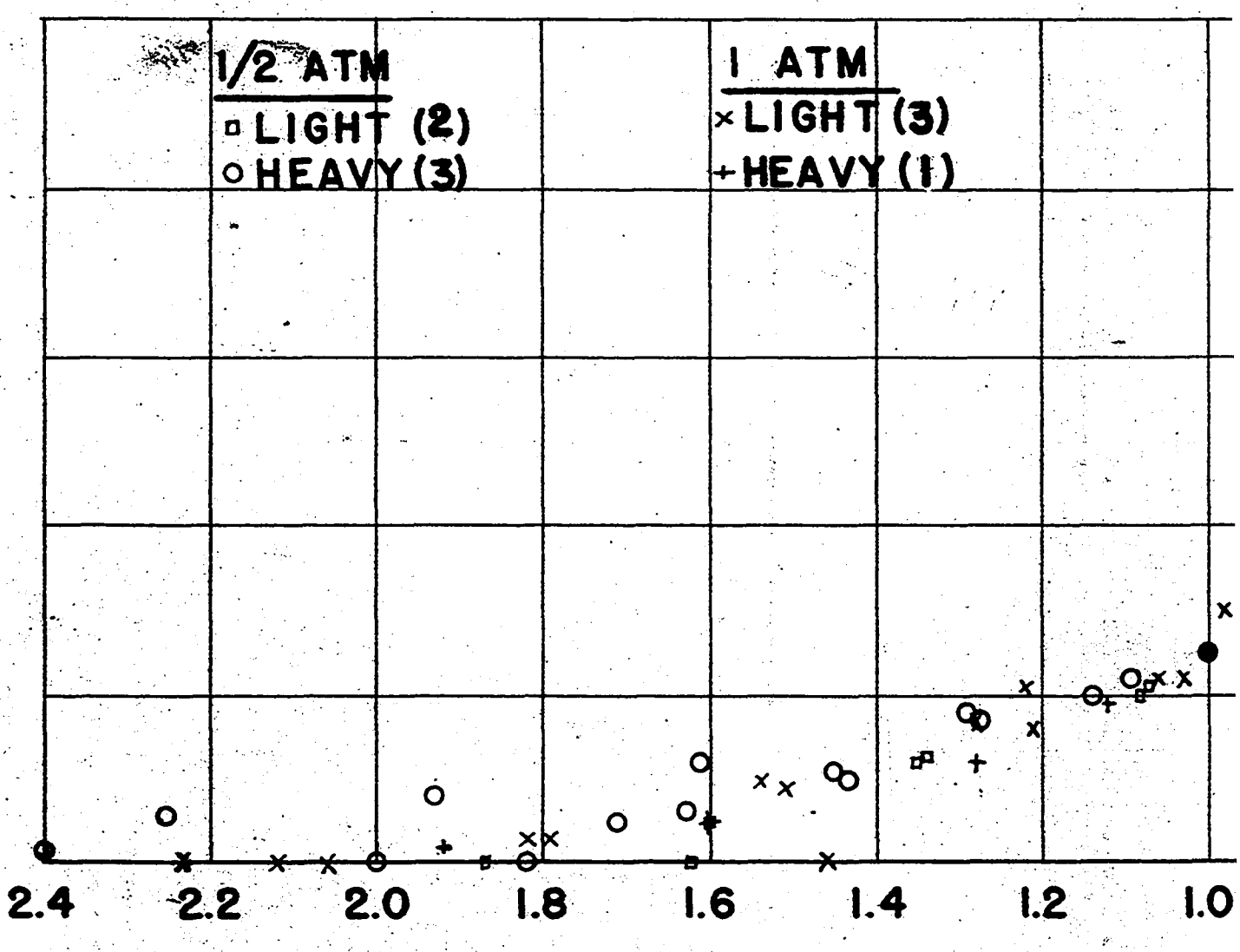

Fig. 14. Fission fragment recombination results for nitrogen. The numb
plotted is indicated.

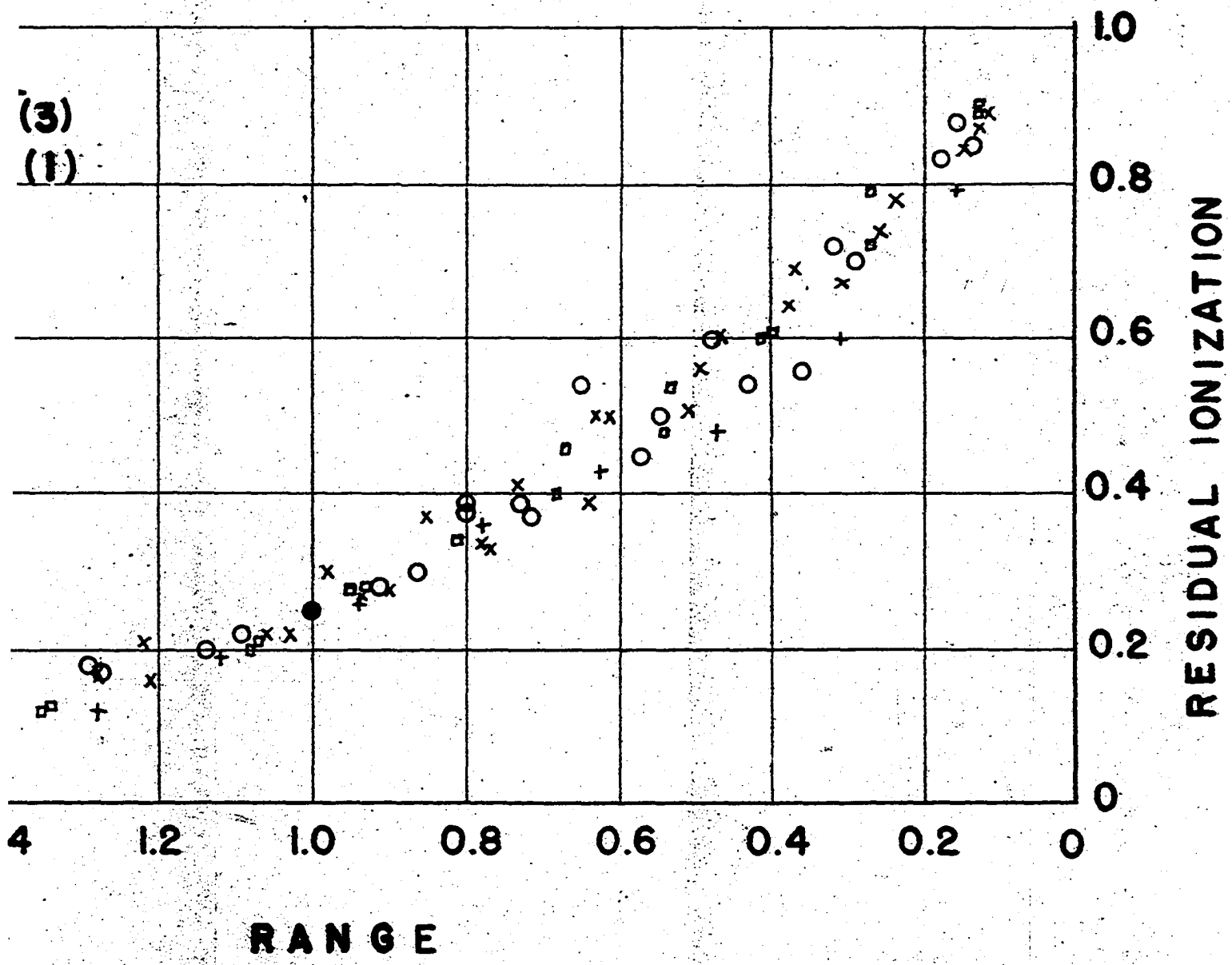

r nitrogen. The number of photographs
ated.

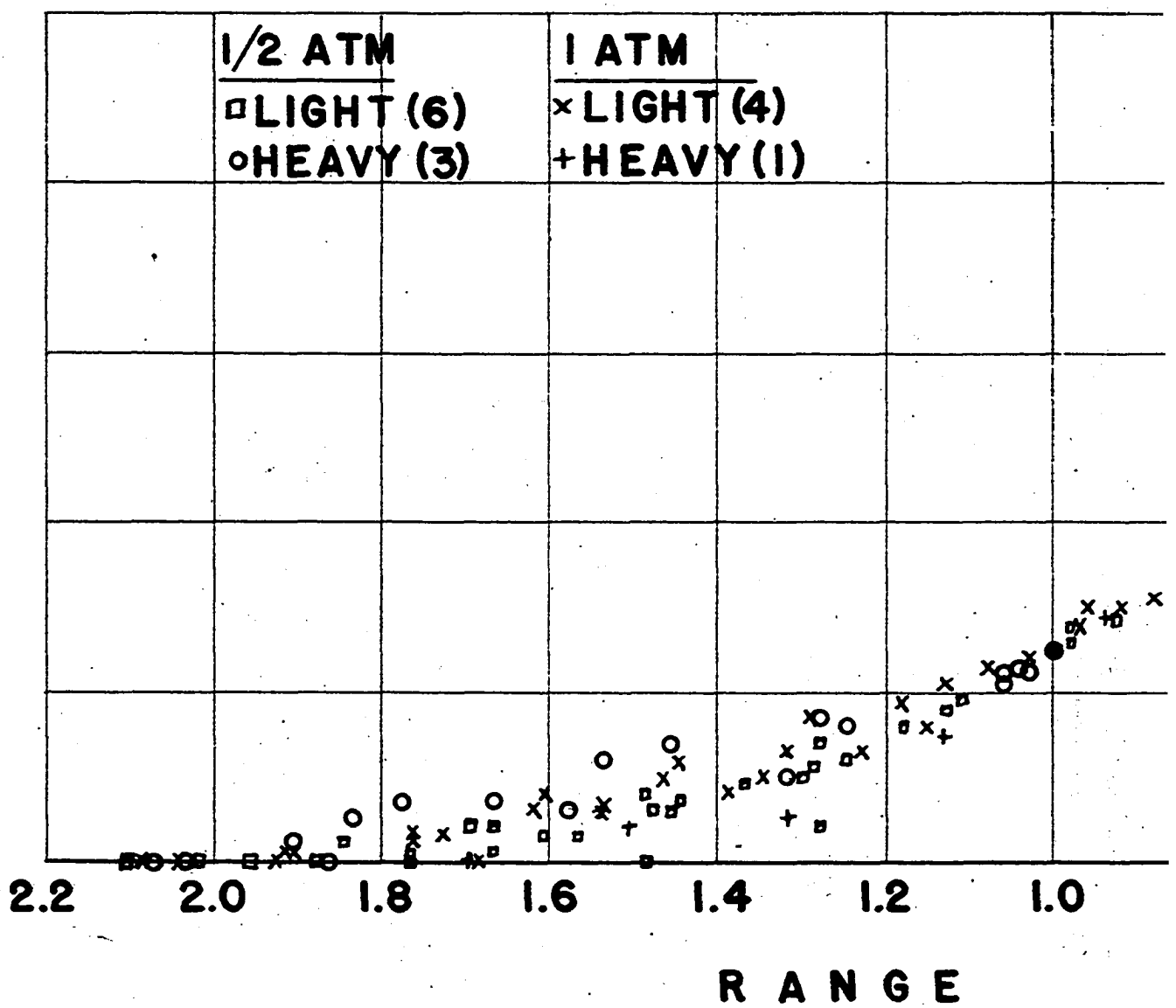

Fig. 15. Fission fragment recombination results for argon. T
is indicated.

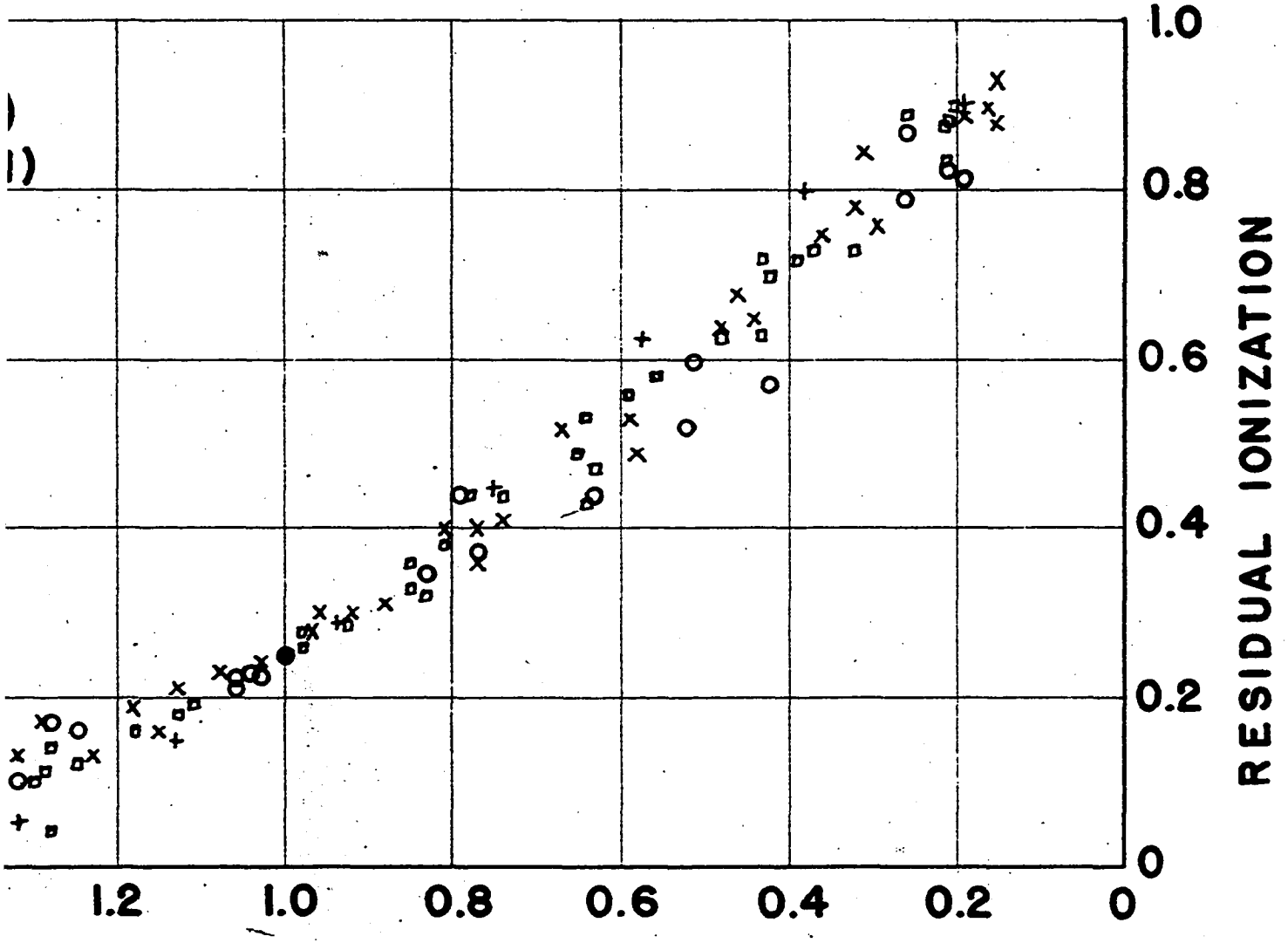

A N G E

ion results for argon. The number of photographs plotted indicated.

the previous section. The U^{235} source was 3/4 in. in diameter so that the fragment ranges for both pressures were within the effective volume of the chamber. Because of the smaller source area, the U^{235} content of the film was made 3.3 mg/cm^2. The U^{235} source was made with the same technique used for natural uranium, except that the plate was brushed rather than dipped. The neutron source was placed on top of the ionization chamber 2.4 cm from the uranium, and the chamber was surrounded by paraffin. The fission rate was about six per hour. Although the energy lost in the uranium was undesirably great, any large distortions due to variations in the proportionality factor between recombination and ion density would have been detected.

Only nitrogen, helium, and argon of the gasses tested had sufficiently low recombination to be useful in the electron collection equipment. Fragments emitted at grazing angle to the high voltage electrode were used to give a measure of the electron diffusion radius for these gasses. Ideally, the dV_c/dt waveform from these fragments would have been rectangular. Actually, because of diffusion and the finite Δt, the trailing edge had an appreciable fall time. Measurements were made of minimum fall times for fission fragments with a 3.81-cm electrode separation and 10-12 μsec. electron collection times.

Diffusion in nitrogen was not measurable; the fall time was essentially Δt. Diffusion in helium was roughly 0.06 cm and in argon about 0.33 cm, where these measurements corresponded to the diffusion distances at which the electron density was about 1/3 the density at the center of the column. On the range-ionization curves this distance corresponded to the difference in range between the point with maximum slope and the point with 1/3 this maximum slope. In the case of argon, in which measurements were the most accurate, it was apparent that a few low amplitude signals had diffusion as low as 0.24 cm. A possible explanation of these few cases is that they represent fragments for which the densest ionization was in the uranium source, and that diffusion increases with electron density because of electrostatic repulsion.

These measurements confirmed the association of diffusion and agitation velocities. The effect of diffusion on the range-ionization data is considered in more detail in the Discussion section.

Range-Ionization Measurements

As mentioned previously, the time duration of the range-ionization waveform is proportional to $\cos \theta$. In order to minimize amplifier and differentiator distortions,

waveforms chosen for analysis were of fragments emitted nearly perpendicular to the chamber electrodes. During the single chamber range-ionization experiment, chamber fillings of helium, nitrogen, and argon were used with different fields. For each of these conditions about 70 fissions were photographed, of which about fifteen of each group were analyzed. The spectrum of total ionization for all the fragments was, for each experimental condition, the familiar double humped distribution curve. Because of poor statistics and the thick source the resolution of heavy and light fragments was not good. Fragments of doubtful identity were not analyzed.

Waveforms were projected by a microfilm reader on graph paper, and coordinates along the curve were recorded. Corrections were made only for obvious excursions of noise, so the data included many of the noise fluctuations. Since the range-ionization curve asymptotically approached zero residual ionization, the determination of total range was difficult. In the comparison of data all ranges were normalized to unity at 25 percent of total ionization, and total ionizations were normalized to unity.

The range-ionization points in Fig. 16 are of seven light and eight heavy fragments stopped in 810 mm Hg of

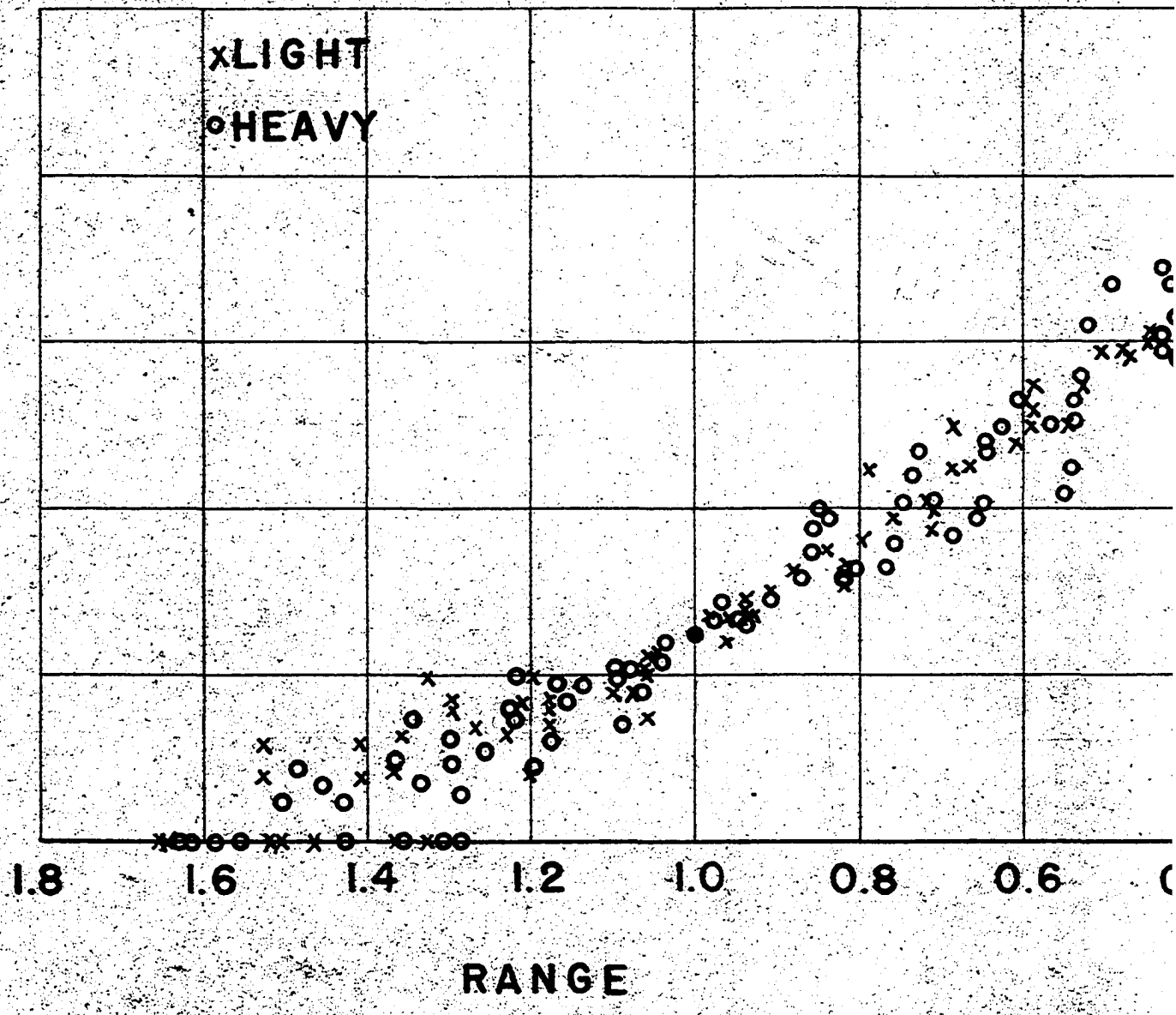

Fig. 16. Range-ionization of fission fragments in nitrogen.

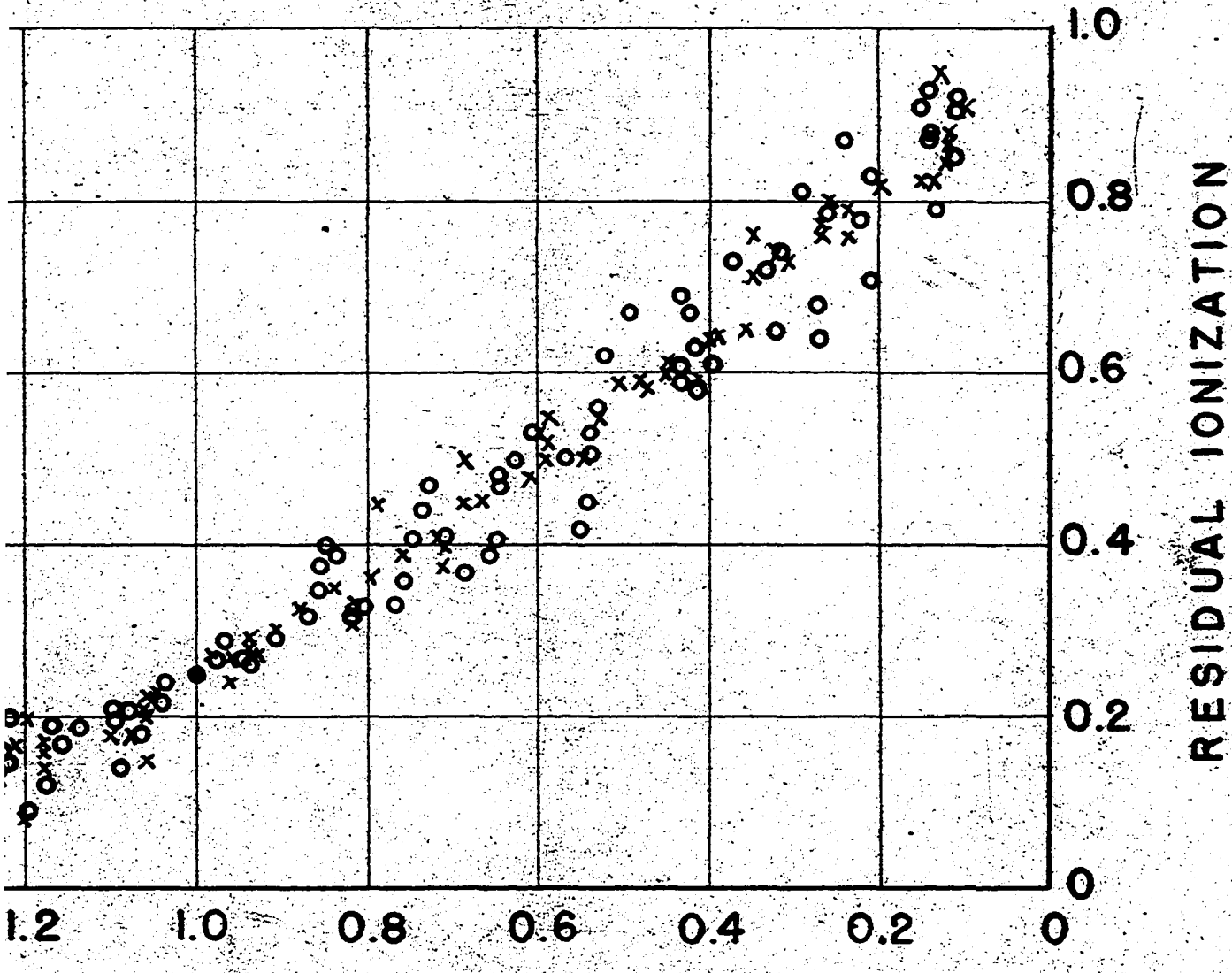

ANGE

ation of fission fragments in nitrogen.

nitrogen purified for 12 hours. About an hour of gas purification was found to decrease the electron collection time of a fresh filling by 25 percent to a stable time of 14 microseconds. The field was 29 V/cm between electrodes of 3.81-cm separation. Fragments were stopped in about one-half this distance.

When helium at 2300 mm Hg was used as a stopping gas the data of Fig. 17 were obtained. Points are of seven light and eight heavy fragments. Little change of collection time was noted during a 12 hour period of purification before data were taken. The same plate separation was used, but a field of 184 V/cm was necessary for a collection time of 14 microseconds. The maximum range of fragments was almost the plate separation.

The points along the range-ionization curves of nine light and eight heavy fragments stopped in 810 mm Hg of argon are plotted in Fig. 18. The argon was purified for 20 hours before data were taken. Little change in collection time was noted. With 3.81-cm electrode separation and a field of 79 V/cm the collection time was 12 microseconds. Fragment ranges were about one-half the electrode separation.

Typical photographs of light fragment waveforms are reproduced in Figs. 19-21 for the three stopping gasses. Since noise was constant, the signal/noise ratios for

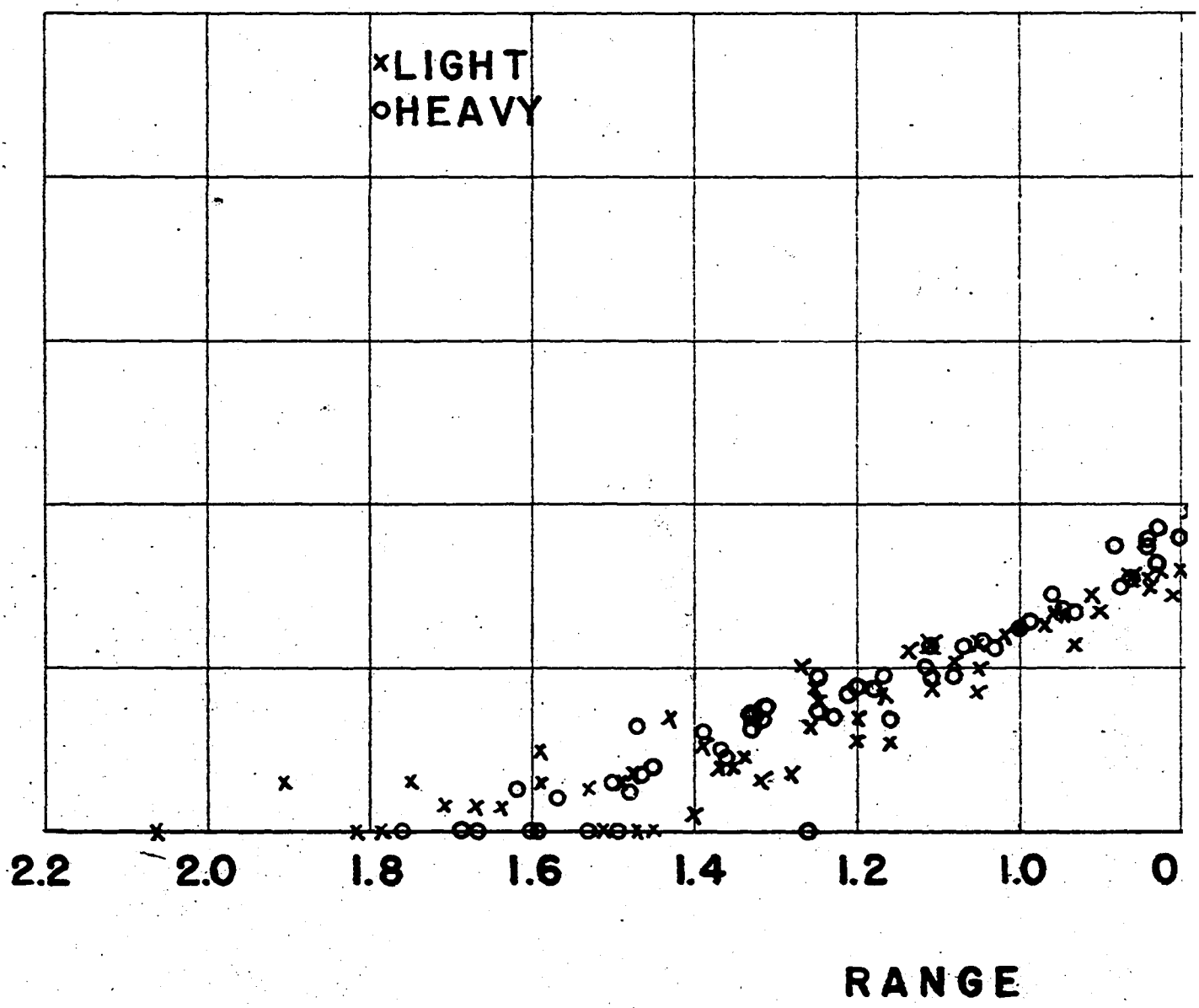

Fig. 17. Range-ionization of fission fragment

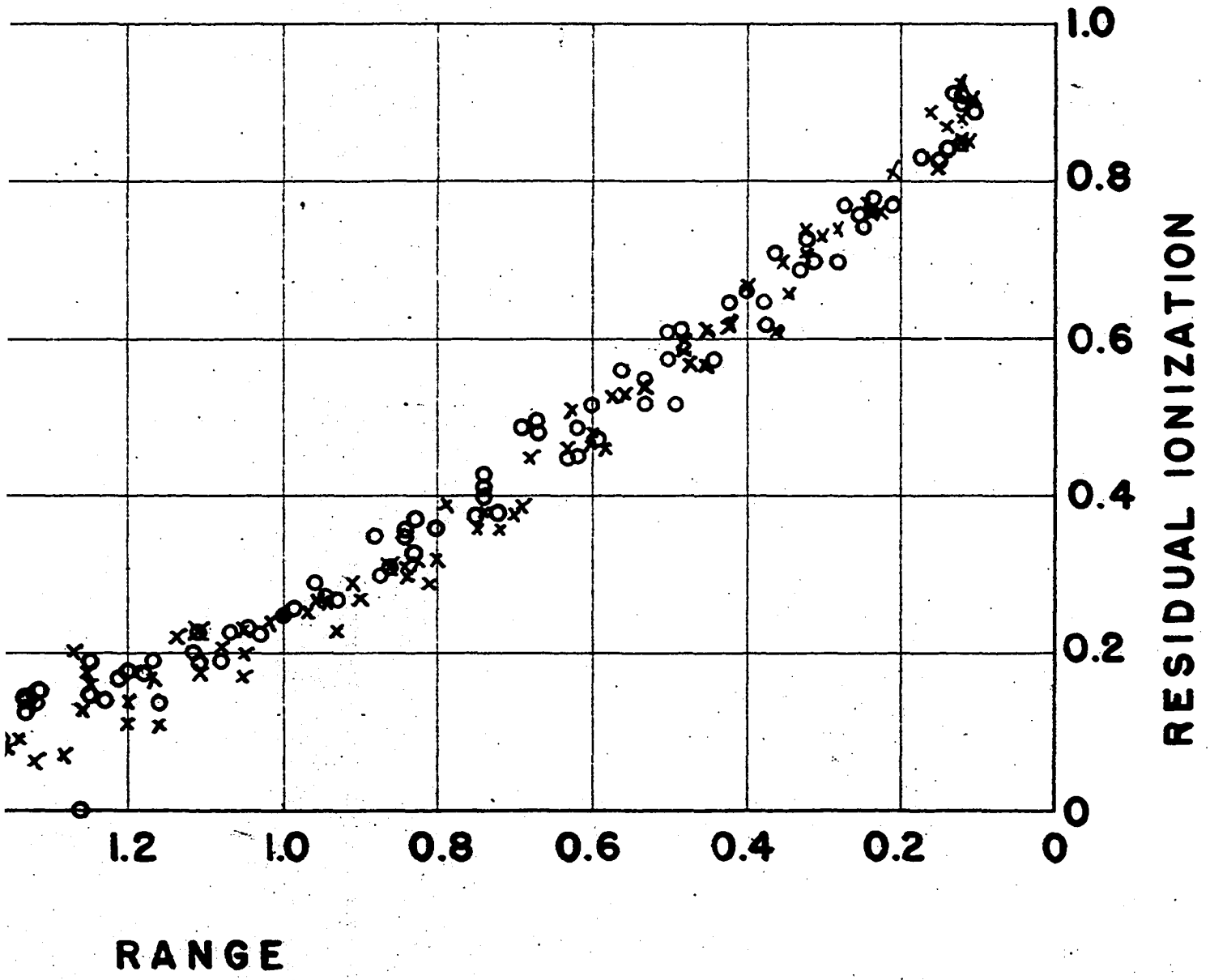

onization of fission fragments in helium.

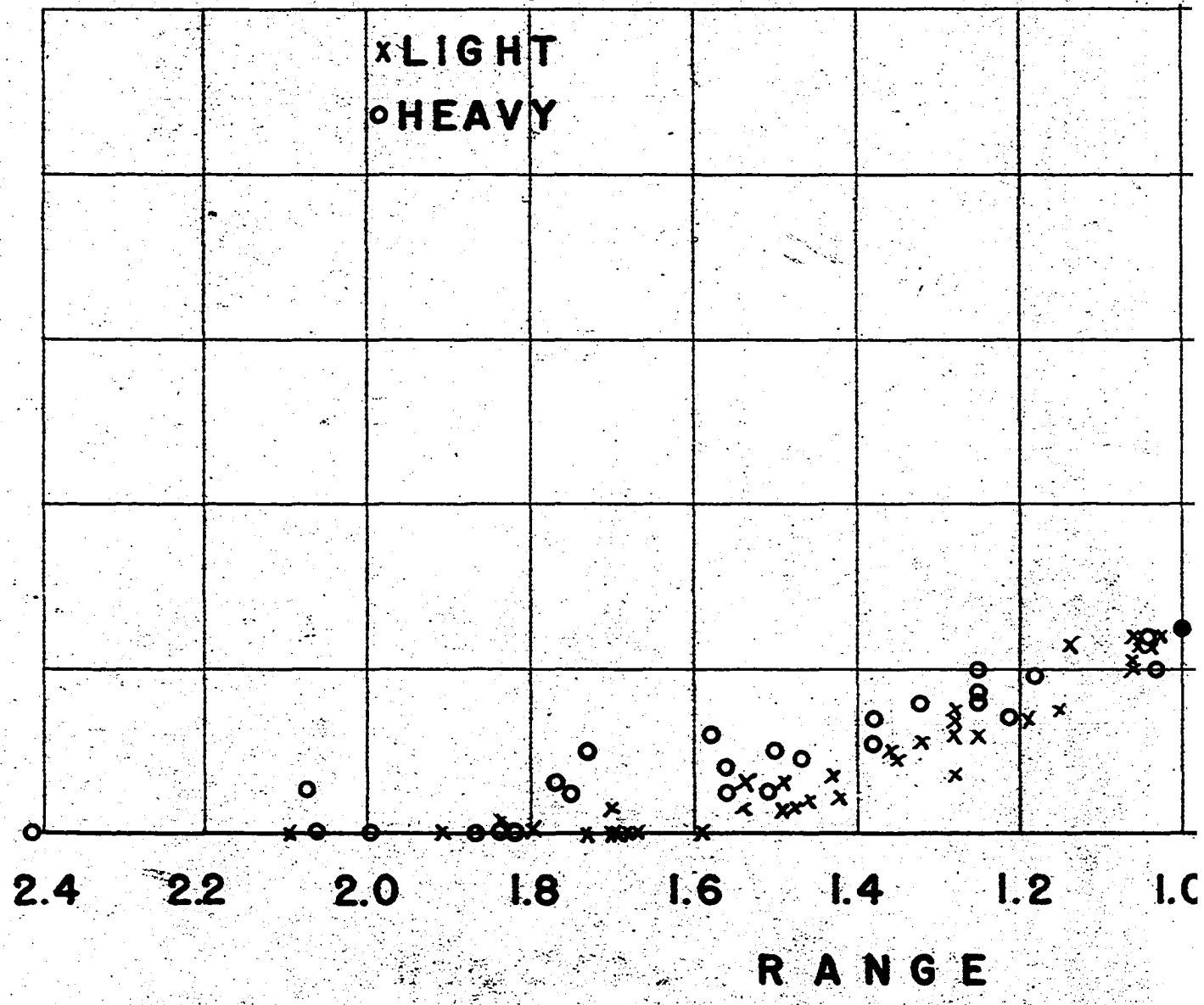

Fig. 18. Range-ionization of fission fragments in argon.

G E

in argon.

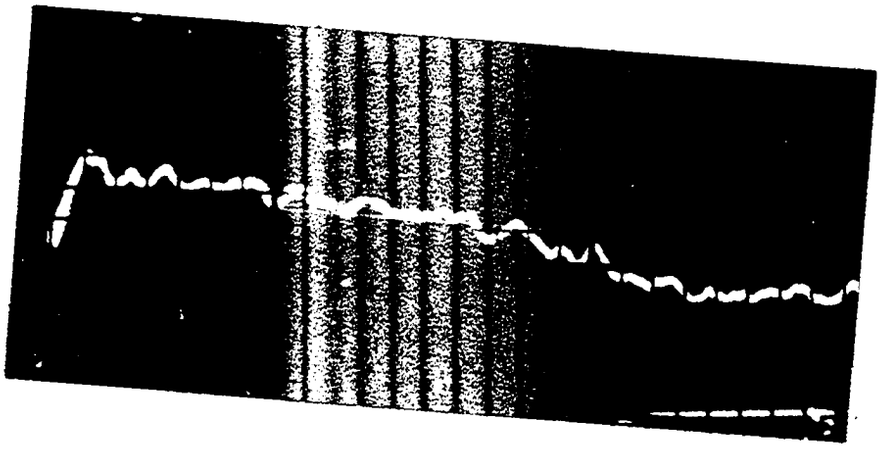

Fig. 19. Oscilloscope waveform of a light fragment in nitrogen.

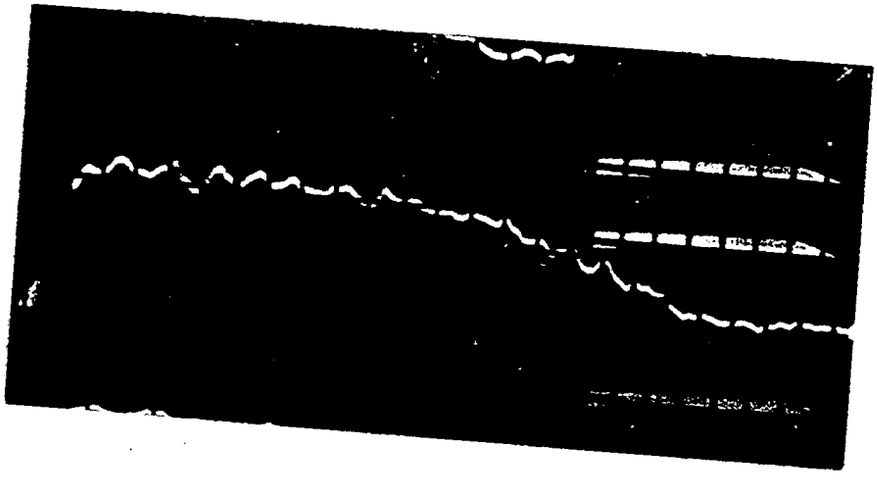

Fig. 20. Oscilloscope waveform of a light fragment in helium.

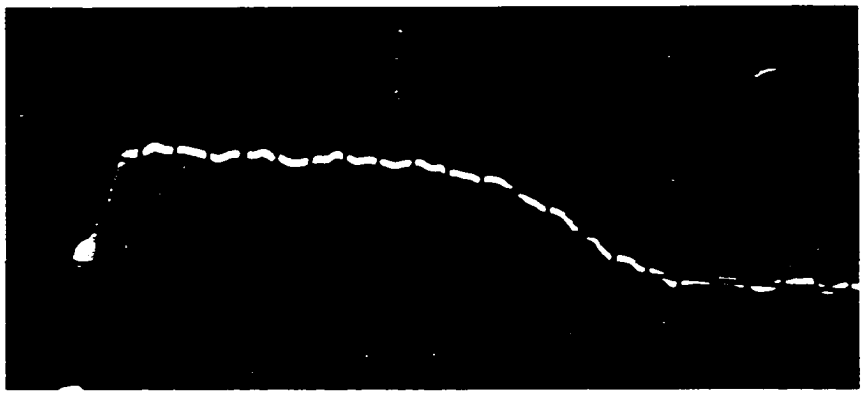

Fig. 21. Oscilloscope waveform of a light fragment in argon.

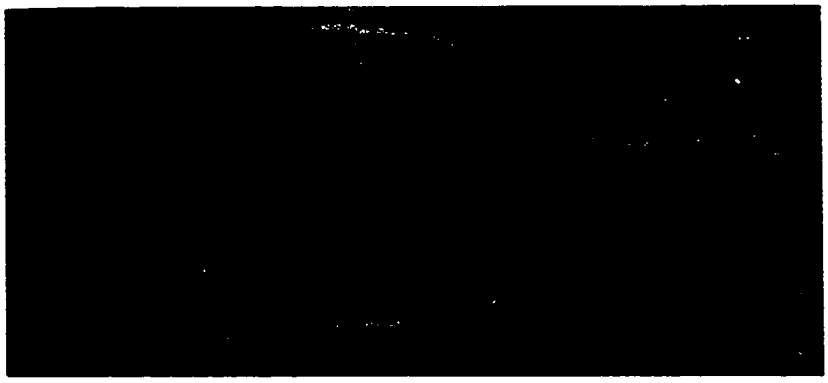

Fig. 22. Dual beam oscilloscope waveforms of a fragment pair. The waveform from the light fragment amplified by the Model 500 and 1000 amplifiers is on the upper trace. The waveform from the heavy fragment amplified by the Model 100 set at about 25 percent greater gain and opposite polarity is on the lower trace.

heavy fragments were lower. Time measurements were obtained from the 0.1-in. superimposed grid and the sweep calibration of 0.15 μsec./in.

The double ionization chamber was filled to 810 mm Hg of argon and fields of 79 V/cm were used with 3.81-cm electrode separations. In Fig. 21 are typical waveforms from the double chambers, where the sweep deflection sensitivities were about 0.35 μsec./in. The upper signal was from the Model 500 and 1000 amplifiers and the lower signal from the Model 100 amplifier. Because of the difficulty in equalizing gains, the Model 100 amplifier had about 25 percent greater gain than the Model 500 and 1000 amplifiers. With this taken into account, the upper waveform in Fig. 22 was identified as a light fragment and the lower waveform as a heavy fragment.

RANGE-IONIZATION DISCUSSION

Because of the greater density of fission fragment ionization, the alpha-particle recombination experiment did not directly indicate the extent of the recombination of ionization from fission fragments. It did indicate the relative recombination in various gasses. Argon data taken by Lassen[3] gave fission fragment ionization as a function of the field strength. His results indicated that, under the experimental conditions employed in the present electron collection experiment, recombination was appreciable even in argon, which is expected to have the lowest recombination of the gasses in Table III.

In the electron collection experiment the signal/noise ratio for nitrogen was considerably lower than for helium or argon, as seen by comparing the photograph in Fig. 19 with those in Figs. 20 and 21. This lower ratio was largely a consequence of the greater recombination in nitrogen. The lower signal/noise ratio resulted in a greater scattering of the nitrogen data in Fig. 16 than in the helium data of Fig. 17. Of equal importance in the quality of the data was the possibility that recombination was not proportional to ion density. Although the results were not conclusive, the fission fragment recombination experiment indicated no distortion of data arrising from this process.

Inspection of the range-ionization data plotted in Figs. 16-18 indicates no difference in the data of light and heavy fragments. Curves best fitting these data are compared in Fig. 23 along with points from the experimental results of Sherr and Peterson[6] and the calculated results of Knipp and Teller[27] for average light and heavy fragments stopped in argon. The results of Knipp and Teller agree well with the argon data of Lassen.[3]

Reasonable explanations can be made for some of the disagreements apparent in Fig. 23. The shorter range of the present data is probably due to an inability to measure signals below the noise level, such as are encountered near the end of the range. The slight difference between the present argon data and that of Sherr and Peterson is probably due to differences in recording the curve near zero range. As seen by the argon waveform in Fig. 21 the curve asymptotically approaches complete ionization in this region. The uncertainty of the point of zero range probably lead to this difference in data and to the scattering of argon data in Fig. 18. The question of whether heavy and light fragments have the same range-ionization curve is to be discussed in connection with

---

[27] J. K. Knipp and E. Teller (private communication).

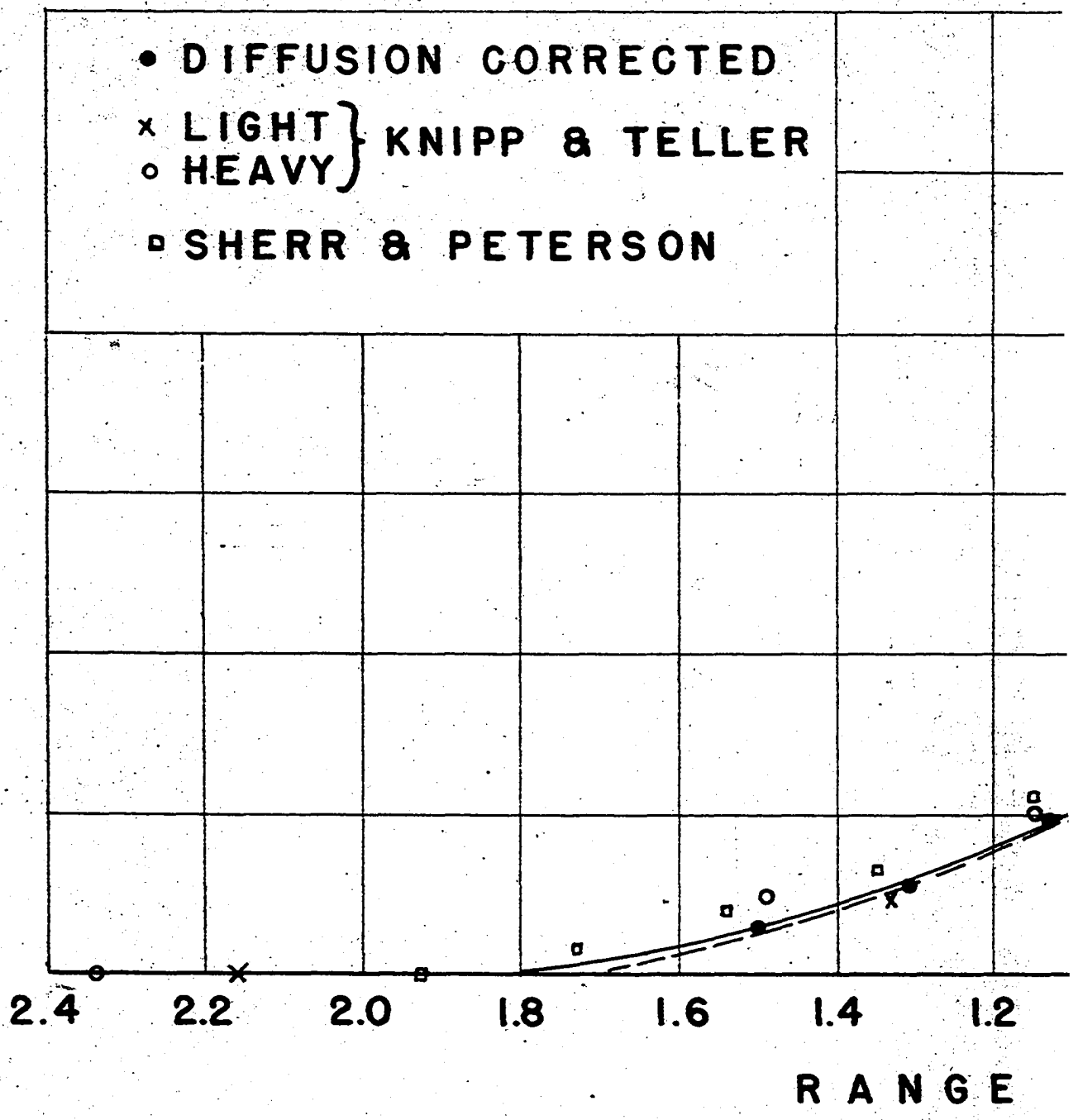

Fig. 23. Comparison of fission fragment range-ioniz

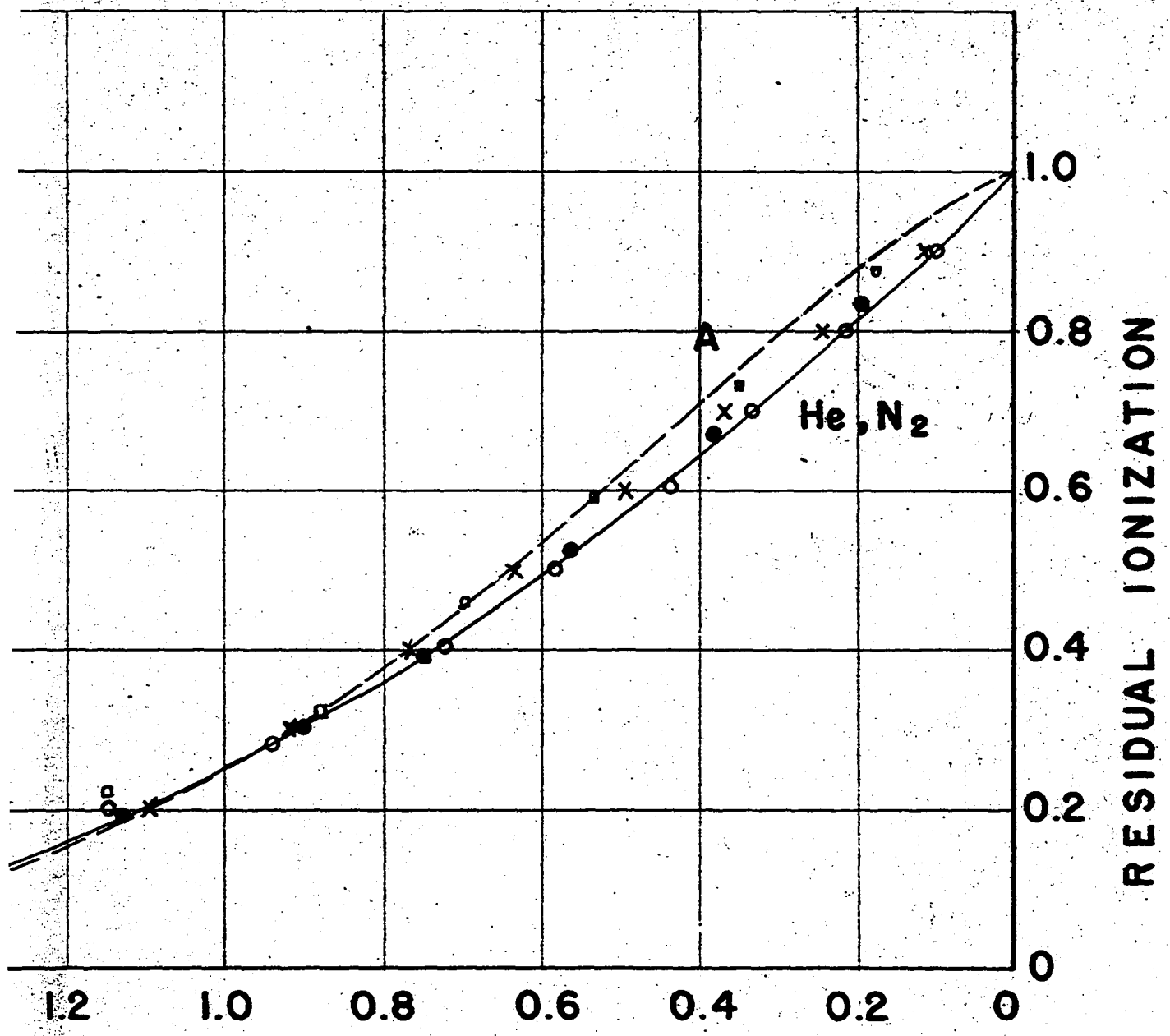

G E

nge-ionization data.

differentiator errors. The contribution of diffusion towards the shape of the argon range-ionization curve is also to be discussed.

In order to evaluate the effect of differentiator errors for different waveforms, Lassen's experimental data of ionization rate, which are different for heavy and light fragments, are used. With the total range normalized to unity these ionization rates closely follow the curves $(1-r)$ and $\left[2(1-r)-(1-r)^2\right]$ for the heavy and light fragments, respectively. Integrating twice we obtain $(1-r)^3/6$ and $\left[4(1-r)^3-(1-r)^4\right]/12$ as the corresponding expressions for V_c. If the substitution $t = 1-r$ is made, the differentiator error is expressed by $(\frac{\Delta V_c}{\Delta t} - \frac{dV_c}{dt})$, where $\Delta V_c/\Delta t$ is given by Eqn. (14). With $V_c = t^3/6$ the differentiator error is composed of a constant and a term linear with t. On the other hand, with $(4t^3-t^4)/12$ an additional term quadradic in t is obtained. The normalization used in compiling the $\Delta V_c/\Delta t$ data eliminates the constant and linear term errors, but not the quadradic term error.

With the data normalization used and with the ionization rate obtained by Lassen, the differentiator error for heavy fragments is seen to be zero. However, the same conditions for light fragments lead to the differentiator error shown in Fig. 24, where the total range and the

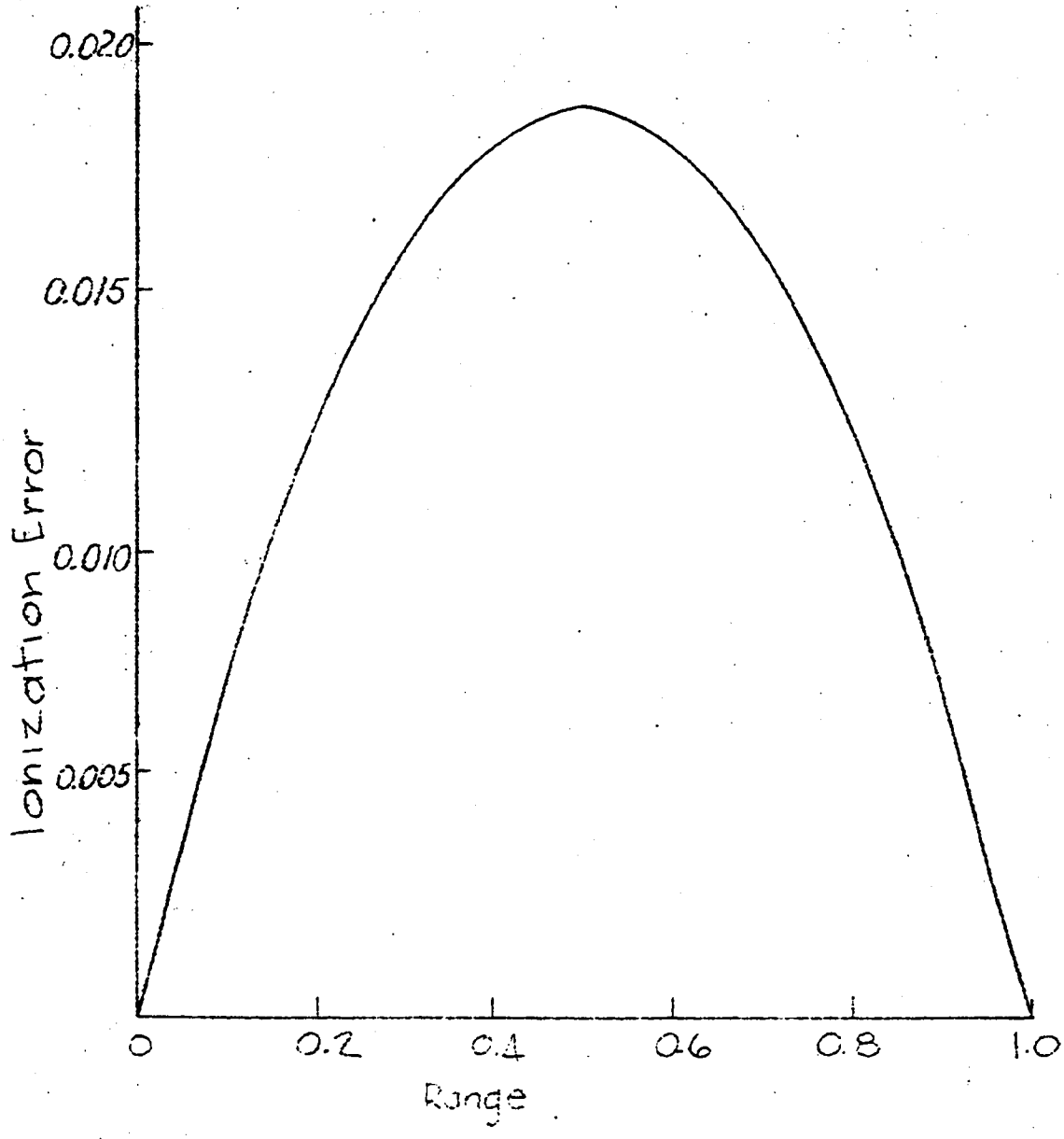

Fig. 24. Possible differentiator error for light fragments in argon. The error curve is calculated from the Lassen ionisation data and $\Delta t/t = 0.1$.

total fragment ionization are normalized to unity. This error added to the present data raises the range-ionization curve of the light fragment, but by roughly one-fifth the amount needed for agreement with Lassen and with Knipp and Teller. It is not inconceivable that the present experimental results contain the additional light and heavy fragment difference in the scattering of data.

With a knowledge of the electron diffusion as a function of collection time, it is possible to calculate the effect of diffusion on a given configuration of ionization. In order to investigate the diffusion effect, the linear $\sigma(x)$ found by Lassen for heavy fragments in argon is used with the diffusion equation of Rossi and Staub[26] and the diffusion measurement for argon given in the last section. When diffusion to the high voltage electrode is neglected, the original ionization distribution $\sigma(x)$ is diffused into the collected ionization distribution $\sigma'(x')$ expressed by

$$\sigma'(x') = \int_{x_1}^{\ell} \sigma(x)\, D(x,x')dx \quad , \tag{15}$$

where x_1 is the end of the fragment range and $D(x,x')$ is the diffusion function. The diffusion function is of

the form

$$D(x,x') \sim \exp\left[-\left(\frac{x - x'}{L\sqrt{x/\ell}}\right)^2\right], \qquad (16)$$

where L is the diffusion distance for $x = \ell$. When Eqn. (15) is graphically solved using the experimental argon values of L = 0.33 cm and $x_1 \cong \ell/2$ and the Lassen heavy fragment $\sigma(x)$, a $\sigma'(x')$ is obtained which leads to the normalized dV_c/dt indicated by points in Fig. 23.

According to this analysis, diffusion has a very small effect on the argon range-ionization data. Furthermore, on the basis of the diffusion distances measured for nitrogen and helium, diffusion in these gasses is expected to be negligible. It appears that the difference between the helium and nitrogen range-ionization curve and the argon curve can not be explained by diffusion alone. This agrees with the results of Lassen for various gasses.

Because of the poor statistics of the double chamber data, analysis is best made by comparison with other data. In Fig. 25 are shown characteristic range-energy curves in argon as a function of fragment mass. These curves are constructed from the data of several experiments. The data used are the range-ionization curve of the present data, the ionization-mass data of Brunton and Hanna,[15]

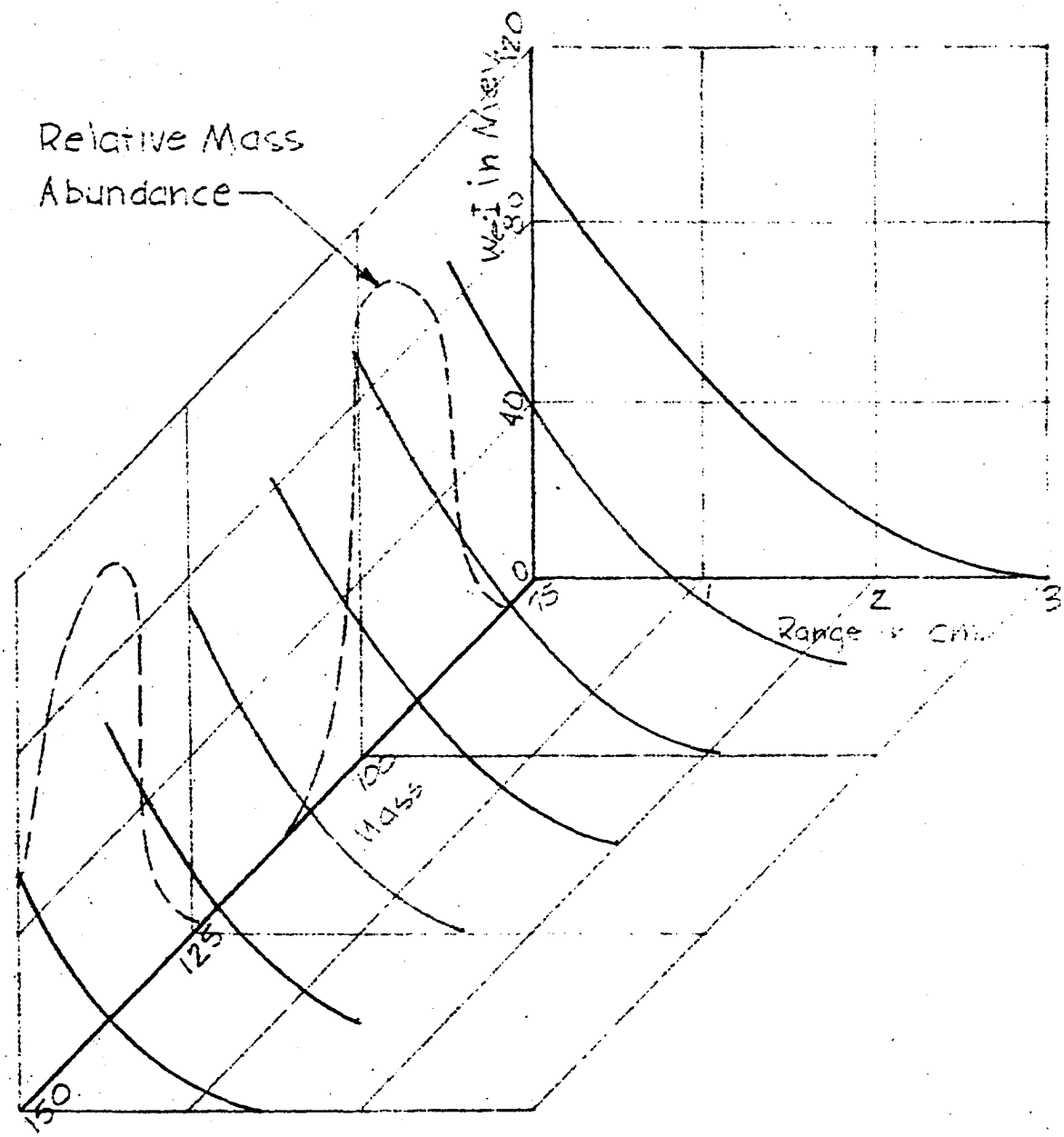

Fig. 25. Dependence of range-ionization curve on fission fragment mass.

and the mass-range data of Katcoff, Miskel, and Stanley.[28] The ranges of the last experiment are normalized to the average argon ranges of Lassen. The data of the double ionization chamber experiment were in accord with Fig. 25.

---

[28] S. Katcoff, J. A. Miskel, and C. W. Stanley, Phys. Rev. 74, 631 (1948).

SUMMARY AND CONCLUSIONS

An investigation of the range-energy properties of fission fragments was undertaken by measuring range-ionization with the electron collection method. In order that these data could be converted to range-energy data, a theoretical investigation of the energy/ionization ratio was undertaken.

The range-ionization data for light and heavy fragments in nitrogen and helium all gave the same curve. Light and heavy fragments in argon gave the same range-ionization curve, which differed from the nitrogen and helium curve. This difference was partially due to high electron diffusion in argon. Errors of electronic differentiation tended to reduce the possible difference between curves of heavy and light fragments.

Simultaneous range-ionization data for both fragments of a pair were obtained from a double ionization chamber. The relatively few data obtained agreed with expectations.

The following conclusions are made as a result of these investigations:

(1) A reasonable interpretation of the results of the energy-ionization study is that the energy/ionization ratio for electronic collisions w_e is constant, but about 1.9 Mev of light fragment energy and 3.4 Mev of heavy fragment

energy lost in nuclear collisions does not appear as ionization.

(2) Effects of electron diffusion and ion pair recombination lower the quality of the range-ionization data obtained by the electron collection method. Diffusion appreciably effects the argon data. Recombination makes the signal/noise ratio with nitrogen undesirably low and with hydrogen and carbon dioxide prohibitively low. The use of helium seems to be a compromise; neither recombination nor diffusion are objectionable.

(3) The electron collection method is not well suited for distinguishing between the nearly alike range-ionization curves of heavy and light fragments.

(4) The data indicated that the range-ionization curves for helium and nitrogen are the same, but this curve differs from the curve for argon.

(5) The data from a double ionization chamber provide significant information on fission fragments only when they are in large quantity.

ACKNOWLEDGEMENTS

The author is indebted to Prof. J. K. Knipp for suggesting the experimental problem and for his many criticisms and suggestions on the energy-ionization investigation. An equal indebtedness is owed Prof. G. H. Miller for his ever present advice and encouragement. Mr. D. Curtis provided helpful advice on thin Zapon films.